RSC Advances

ROYAL SOCIETY OF CHEMISTRY

PAPER

View Article Online
View Journal | View Issue

Check for updates

Cite this: *RSC Adv.*, 2022, **12**, 22385

Design, synthesis and biological evaluation of benzo-[*d*]-imidazo-[2,1-*b*]-thiazole and imidazo-[2,1-*b*]-thiazole carboxamide triazole derivatives as antimycobacterial agents†

Surendar Chitti,[a] Kevin Van Calster,[b] Davie Cappoen,*[b] Adinarayana Nandikolla,[a] Yogesh Mahadu Khetmalis,[a] Paul Cos,[b] Banoth Karan Kumar,[c] Sankaranarayanan Murugesan[c] and Kondapalli Venkata Gowri Chandra Sekhar*[a]

In the search for new anti-mycobacterial agents, we revealed the importance of imidazo-[2,1-*b*]-thiazole and benzo-[*d*]-imidazo-[2,1-*b*]-thiazole carboxamide derivatives. We designed, *in silico* ADMET predicted and synthesized four series of novel imidazo-[2,1-*b*]-thiazole and benzo-[*d*]-imidazo-[2,1-*b*]-thiazole carboxamide analogues in combination with piperazine and various 1,2,3 triazoles. All the synthesized derivatives were characterized by ^{1}H NMR, ^{13}C NMR, HPLC and MS spectral analysis and evaluated for *in vitro* antitubercular activity. The most active benzo-[*d*]-imidazo-[2,1-*b*]-thiazole derivative **IT10**, carrying a 4-nitro phenyl moiety, displayed IC_{90} of 7.05 μM and IC_{50} of 2.32 μM against *Mycobacterium tuberculosis* (Mtb) H37Ra, while no acute cellular toxicity was observed (>128 μM) towards the MRC-5 lung fibroblast cell line. Another benzo-[*d*]-imidazo-[2,1-*b*]-thiazole compound, **IT06**, which possesses a 2,4-dichloro phenyl moiety, also showed significant activity with IC_{50} 2.03 μM and IC_{90} 15.22 μM against the tested strain of Mtb. Furthermore, the selected hits showed no activity towards a panel of non-tuberculous mycobacteria (NTM), thus suggesting a selective inhibition of Mtb by the tested imidazo-[2,1-*b*]-thiazole derivatives over the selected panel of NTM. Molecular docking and dynamics studies were also carried out for the most active compounds **IT06** and **IT10** in order to understand the putative binding pattern, as well as stability of the protein–ligand complex, against the selected target Pantothenate synthetase of Mtb.

Received 27th May 2022
Accepted 3rd August 2022

DOI: 10.1039/d2ra03318f

rsc.li/rsc-advances

1 Introduction

According to the report submitted by the world health organization, globally, 1.4 million people died from tuberculosis (TB) in 2019; almost one-fourth of the world's population is infected with its etiological agent, the weakly Gram-positive *Mycobacterium tuberculosis* (Mtb). TB is a pulmonary infectious disease spread by aerosols and ranks among the top 10 causes of mortality worldwide.[1] TB is curable and preventable, if the patient takes appropriate treatment and precautions. Patients with smear-positive pulmonary TB (without HIV co-infection) have a 50–60% risk to die within 5 years without treatment while 20–25% achieve spontaneous resolution.[2] The remainder of these patients will develop a Latent TB Infection (LTBI), a state of persistent Mtb infection without evidence of clinically manifested active TB. However, people with LTBI risk developing active TB when they become immunocompromised later in life. Hence, development of a super-selective drug candidate to cure or prevent TB is imperative.[3] Nitrogen, oxygen, and sulphur nucleus-based heterocycles are important compounds in medicinal chemistry.[4–9] Many biologically active pharmaceutical ingredients are constructed with fused five-membered bicyclic rings. Hence fused heterocyclic moieties became valuable in novel drug discovery and medicinal chemistry. Imidazo [2,1-*b*]-thiazoles are reported to exhibit antitubercular,[10] antibacterial,[11] antifungal,[12,13] anticancer,[14] antiviral,[15] anti-inflammatory,[16] anthelmintic,[17] antihypertensive,[18] cardiotonic,[19,20] and insecticidal,[21] properties. Benzo-[*d*]-imidazo-[2,1-*b*] scaffold is often observed in several active pharmaceutical ingredients and bioactive molecules. Compounds containing benzo-[*d*]-imidazo-[2,1-*b*] skeleton have antimicrobial,[22] anticancer,[23] antibacterial,[24] and antiallergic properties.[25] In addition, benzo-

[a]Department of Chemistry, Birla Institute of Technology and Science, Pilani, Hyderabad Campus, Jawahar Nagar, Hyderabad-500 078, Telangana, India. E-mail: kvgc@hyderabad.bits-pilani.ac.in; kvgcs.bits@gmail.com; Tel: +91 40 66303527

[b]Laboratory of Microbiology, Parasitology and Hygiene, Department of Pharmaceutical Sciences, University of Antwerp, Universiteitsplein 1, 2610, Wilrijk, Belgium. E-mail: davie.cappoen@uantwerpen.be

[c]Medicinal Chemistry Research Laboratory, Department of Pharmacy, Birla Institute of Technology and Science Pilani, Pilani Campus, Pilani-333031, Rajasthan, India

† Electronic supplementary information (ESI) available. See https://doi.org/10.1039/d2ra03318f

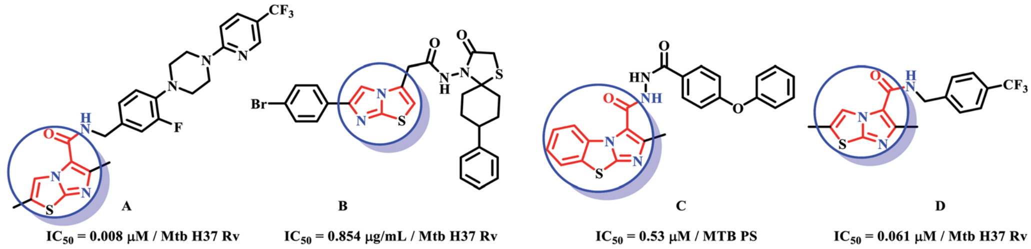

Fig. 1 Structure of imidazo-[2,1-*b*]-thiazole and benzo-[*d*]-imidazo-[2,1-*b*]-thiazole based active antitubercular agents.

[*d*]-imidazo-[2,1-*b*]-thiazole products exhibit a potential role as various kinase inhibitors.[26–29] Imidazo-[2,1-*b*]-thiazole carboxamide derivatives (**A**) also have notable anti-TB activity.[29,30] Imidazo-[2,1-*b*]-thiazole-bearing aza spiro carboxamide derivative **B** of imidazo-[2,1-*b*]-thiazole showed strong antitubercular activity.[31] Samala *et al.* reported anti-TB activity of a few imidazo-[2,1-*b*]-thiazole and benzo-[*d*]-imidazo-[2,1-*b*]-thiazole carboxamide derivatives (**C**) with MIC 3.53 μM and IC_{50} 0.53 ± 0.13 μM.[32] Moraski and group recently reported that novel carboxamide derivatives of imidazo-[2,1-*b*]-thiazole have promising antitubercular activity, among them compound **D** displayed remarkable activity with MIC 0.061 μM and toxicity >100 μM (ref. 33) (Fig. 1).

In medicinal, agrochemical research, and material sciences the triazole analogues play a key role.[34–36] Triazole is an unsaturated five membered heterocyclic compound containing three nitrogen's and two carbons. In recent years, **I-A09** small molecule was identified as a potent mycobacterium protein tyrosine phosphate **B** inhibitor. It carries both benzofuran salicylic acid and 1,2,3-triazole analogue, which have been in clinical use since the last decade and have provided an innovative drug candidate for the treatment of Mtb.[37–39] Recently reported notable active molecules (**E, F, G**) exhibiting antitubercular activity based on the 1,2,3-triazole skeleton are depicted in Fig. 2.[40–42]

Pantothenate synthetase (PS) of Mtb is a homodimer protein which catalyzes the synthesis of pantothenate from D-pantoate and β-alanine. It is the last enzyme present in the pantothenate biosynthesis pathway and has been considered as crucial for the pathogenicity, persistence and survival of Mtb in the host. Generally, pantothenate can be synthesized by microorganisms. In contrast, mammals cannot produce the molecule and need to obtain it from dietary sources. For these reasons, in recent years the enzyme made for an interesting target in developing potential agents against various forms of Mtb.[43–46] Recently, many Mtb PS inhibitors are reported by the researchers, including 2-methylimidazo-[1,2-*a*]-pyridine-3-carboxamide, pyrazole-[4,3-*c*]-pyridine carboxamide, 1-benzoyl-*N*-(4-nitrophenyl)-3-phenyl-6,7-dihydro-1*H*-pyrazolo-[4,3-*c*]-pyridine-5-(4*H*)-carboxamide, imidazo-[2,1-*b*]-thiazole, benzo-[*d*]-imidazo-[2,1-*b*]-thiazole derivatives and one of the widely used first-line antitubercular drug, pyrazinamide.[43,44] Moreover, our group recently offered a critical review on inhibitors of Mtb PS from a medicinal chemist's perspective.[47] Bearing in mind these findings as well as our continuous interest in the field of anti-TB drug discovery, we identified our titled compounds as potential inhibitors of Mtb PS during the molecular docking study.

Piperazine moiety is also well explored for anti-tubercular activity.[32,48–50] Aiming to discover novel antitubercular compounds[35,51] and owing to the importance of these heterocyclics, in this manuscript, we focused on the synthesis of piperazine bearing benzo-[*d*]-imidazo-[2,1-*b*]-thiazole and imidazo-[2,1-*b*]-thiazole scaffolds with various 1,2,3-triazole analogues. Our design strategy is depicted in Fig. 3.

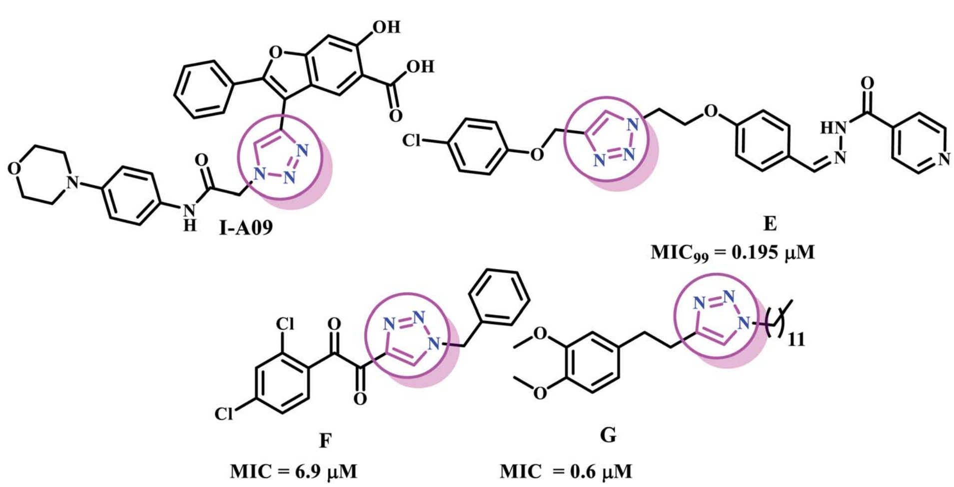

Fig. 2 Structure of 1,2,3-triazole based antitubercular molecules.

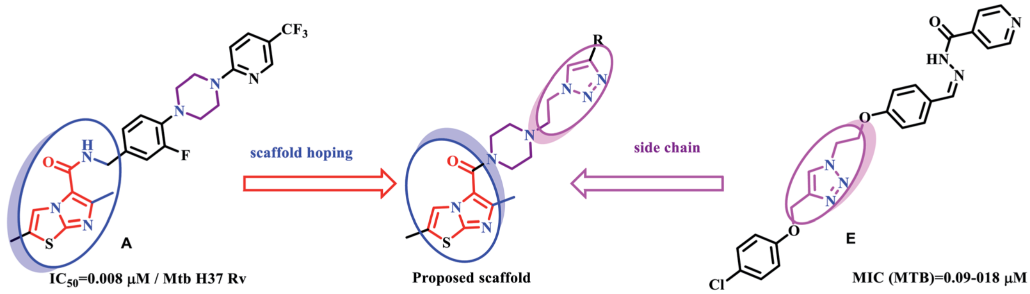

Fig. 3 Scaffold design strategy for the proposed novel antitubercular agents.

2 Results and discussion

2.1 *In silico* prediction of drug-likeness properties

In silico physicochemical and pharmacokinetic parameters of imidazo-[2,1-*b*]-thiazole (**IT01–05**, **IT19–IT27**) and benzo-[*d*]-imidazo[2,1-*b*]-thiazole (**IT06–IT18**) analogues were predicted using the knowledge-based FAF Drugs4 and Swiss ADME software tools to enable the selection of designed analogues that are suitable for further biological evaluation.[52,53] Narrowing the collection to a set of compounds including a high drug-likeness saves wasting money on compounds that could have negative side effects later in the drug research and development process.[54] Table 1 represents the anticipated drug-likeness parameters of each designed hybrid analogues; the prescribed cut-off ranges of each and every parameter that are being followed by 95% of known marketed drugs were added in the footnotes of the table,[49] Other than molecular weight, most of the designed imidazo-[2,1-*b*]-thiazole and benzo-[*d*]-imidazo-[2,1-*b*]-thiazole derivatives met the predicted *n*-octanol values, and the water partition coefficient, hydrogen bond acceptors and hydrogen bond donors' parameters. The values were all within the established limits and validating Lipinski's rule of five. Additionally, the number of atoms was within the acceptable range, enhancing drug-likeness. All the titled imidazo-[2,1-

Table 1 *In silico* predicted physicochemical and pharmacokinetic parameters of the imidazo-[2,1-*b*]-thiazole and benzo-[*d*]-imidazo-[2,1-*b*]-thiazole derivatives

Cmpd.	MW[a]	log P[b]	HBD[c]	HBA[d]	Heavy atoms[e]	Rotatable bonds[f]	log Sw[g]	Solubility forecast index	Oral bioavailability (Veber's rule)
IT01	401.53	3.38	8	5	28	8	−3.92	Good	Good
IT02	477.62	4.25	7	5	34	7	−5.51	Good	Good
IT03	471.66	4.88	13	5	33	13	−5.69	Good	Good
IT04	493.61	3.38	7	6	34	7	−5.03	Good	Good
IT05	472.95	3.60	7	7	32	7	−4.53	Good	Good
IT06	526.44	4.14	5	5	35	5	−6.60	Good	Good
IT07	487.58	4.21	6	6	35	6	−5.46	Good	Good
IT08	502.55	3.48	6	7	36	6	−5.48	Good	Good
IT09	485.60	4.31	5	5	35	5	−5.99	Good	Good
IT10	502.55	3.40	6	7	36	6	−5.48	Good	Good
IT11	492.00	4.17	5	5	34	5	−5.99	Good	Good
IT12	451.59	4.13	8	5	32	8	−5.16	Good	Good
IT13	527.68	4.55	7	5	38	7	−6.74	Good	Good
IT14	521.72	5.10	13	5	37	13	−6.93	Good	Good
IT15	471.58	3.87	6	5	34	6	−5.45	Good	Good
IT16	543.67	3.89	7	6	38	7	−6.25	Good	Good
IT17	523.01	4.00	7	7	36	7	−5.76	Good	Good
IT18	435.55	3.57	6	5	31	6	−4.48	Good	Good
IT19	385.49	3.07	6	5	27	6	−3.24	Good	Good
IT20	421.52	3.29	6	5	30	6	−4.22	Good	Good
IT21	486.39	3.82	5	5	30	5	−5.07	Good	Good
IT22	459.93	3.66	5	6	31	5	−4.93	Good	Good
IT23	459.93	3.66	5	6	31	5	−4.24	Good	Good
IT24	435.55	3.92	5	5	31	5	−4.75	Good	Good
IT25	452.49	2.98	6	7	32	6	−4.24	Good	Good
IT26	441.94	3.43	5	5	30	5	−4.76	Good	Good
IT27	437.52	3.61	6	6	31	6	−4.23	Good	Good

[a] Molecular Weight (MW; 130 to 725). [b] Log partition coefficient between *n*-octanol and water (−2 to 6.5). [c] # hydrogen bond donors (0–6). [d] # hydrogen acceptors (2–20). [e] # Heavy atoms (non-hydrogen) (20–70). [f] Number of rotatable bonds (0–15). [g] Log aqueous solubility (−6.5 to 0.5).

b]-thiazole and benzo-[*d*]-imidazo-[2,1-*b*]-thiazole's predicted aqueous solubility was good. Based on Veber's rule, the imidazo-[2,1-*b*]-thiazole and benzo-[*d*]-imidazo-[2,1-*b*]-thiazole analogues were also considered to have good oral bioavailability.[55] Overall outcomes disclose that the designed imidazo-[2,1-*b*]-thiazole and benzo-[*d*]-imidazo-[2,1-*b*]-thiazole derivatives generally possess drug-like behaviour. Hence, all derivatives were selected for further research.

2.2 Chemistry

To achieve the title derivatives (**IT01–IT27**), we followed a synthetic strategy represented in Scheme 1. The cyclization of compound **1** with ethyl 2-chloro-3-oxobutanoate (**2**) in 1,4-dioxane under reflux condition produced the ethyl 2-methylbenzo-[*d*]-imidazo-[2,1-*b*]-thiazole-3-carboxylate (**3**). The obtained compound **3** was established by ^{1}H NMR. Earlier literature reports also confirm the formation of compound **3**.[29–32,51] A specific singlet peak for the methyl group protons at δ 2.28 ppm was observed. In mass spectroscopy we observed [M + 1] peak at $m/z = 261.2$, confirming the presence of compound **3**. Later, compound **3** was further subjected to ester hydrolysis in presence of LiOH to yield corresponding acid **4**; structure of **4** was confirmed by loss of the ethoxy proton signals and appearance of a broad exchangeable peak at δ 12.08 ppm in ^{1}H NMR. The acid **4** was subjected to amide coupling with *n*-Boc piperazine using HATU as coupling agent and Hunig's base to get the carboxamide **5**, which was confirmed by MS analysis. The carboxamide (**5**) was subjected to Boc deprotection in acidic medium to obtain key intermediate **6**; the absence of Boc protons at 1.49 ppm in ^{1}H NMR confirmed the formation of **6**. *N*-alkylation of **6** with 2-bromoethanol and propargyl bromide in the presence of K_2CO_3 yielded the corresponding *N*-alkylated products (**8** and **11**). Compound **8** was treated with methyl silyl chloride followed by sodium azide to get the compound **9.** The alkylated products (**9** and **11**) finally were reacted with various acetylenes and azides using well-known click chemistry to yield titled 1,2,3-triazole derivatives. In the ESI† we discussed the detailed procedure for each step, while the corresponding analytical data of the final compounds is in Section 1.

TLC (thin-layer chromatography) and ESI mass spectrometry were used to monitor all reactions. The obtained crude product from every step was purified *via* column chromatography using silica gel (mesh size is 100–200) and (10 to 100%) EtOAc : petroleum ether as eluent. All title compounds were subjected to ESI-MS, ^{1}H NMR and ^{13}C NMR for further confirmation of structures.

2.3 Biological evaluation

The titled synthesized compounds, imidazo-[2,1-*b*]-thiazole (**IT01–IT05**, **IT19–IT27**) and benzo-[*d*]-imidazo-[2,1-*b*]-thiazole (**IT06–IT18**) were examined for their antimycobacterial activity against Mtb. A prototype based on a luminescent Mtb H37Ra lab strain (H37Ra^{lux}) was used. As previously reported in the literature, this technique provides a sensitive and repeatable tool, able to substitute enumeration of bacteria by careful plating on agar.[57,58] Antitubercular properties of the synthesized compounds were elucidated by comparing the reduction of luminescence emitted by a culture exposed to the compound to a negative control culture. After seven days of exposure of Mtb H37Ra^{lux} to successive dilutions of the compounds, the

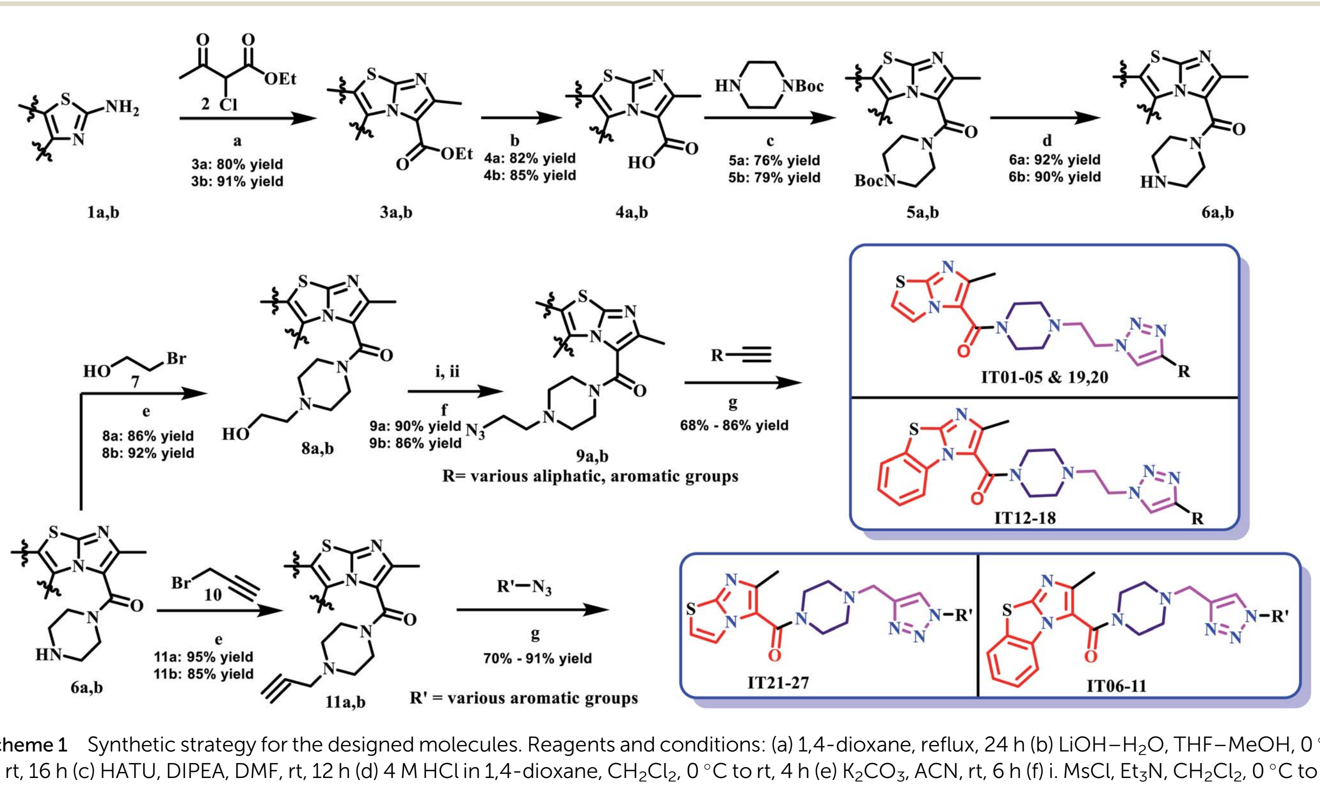

Scheme 1 Synthetic strategy for the designed molecules. Reagents and conditions: (a) 1,4-dioxane, reflux, 24 h (b) LiOH–H_2O, THF–MeOH, 0 °C to rt, 16 h (c) HATU, DIPEA, DMF, rt, 12 h (d) 4 M HCl in 1,4-dioxane, CH_2Cl_2, 0 °C to rt, 4 h (e) K_2CO_3, ACN, rt, 6 h (f) i. MsCl, Et_3N, CH_2Cl_2, 0 °C to rt, 2 h; ii. NaN_3, DMSO, 70 °C, 5 h (g) $CuSO_4 \cdot 5H_2O$, sodium ascorbate, DMF-*t*-BuOH-H_2O (5 : 3 : 2), 0 °C to rt, 12–14 h.

Table 2 Antimycobacterial results of the synthesized imidazo-[2,1-*b*]-thiazole and benzo-[*d*]-imidazo-[2,1-*b*]-thiazole derivatives against H37Ra and MRC-5 strains

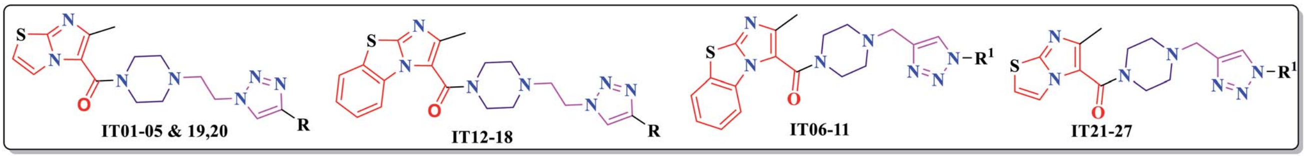

Cmpd.	R	R^1	Mtb H37Ra[lux a] IC_{90} (μM)	Mtb H37Ra[lux a] IC_{50} (μM)	MRC-5[b] CC_{50} (μM)	T.I.[c] CC_{50}/IC_{50}
IT01	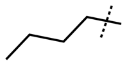	—	52.03	6.12	N.D.[(d)]	N.A.[e]
IT02	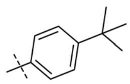	—	12.83	5.20	46.01	8.8
IT03	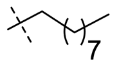	—	10.22	2.88	45.49	15.8
IT04	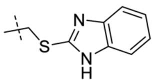	—	14.59	3.94	>128	32.5
IT05	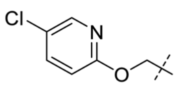	—	>128	49.6	N.D.	N.A.
IT06	—	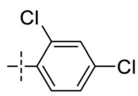	15.22	2.03	N.D.	N.A.
IT07	—	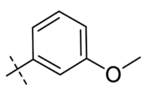	15.36	7.27	N.D.	N.A.
IT08	—	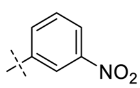	11.81	2.96	>128	43.2
IT09	—	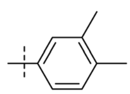	13.49	3.46	>128	37.0
IT10	—	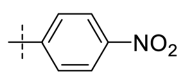	7.05	2.32	>128	55.2
IT11	—	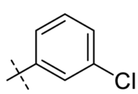	14.46	3.86	29.42	7.6
IT12	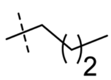	—	62.76	43.67	N.D.	N.A.
IT13	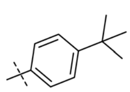	—	7.24	3.19	43.67	13.7
IT14	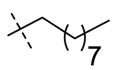	—	27.96	13.07	N.D.	N.A.
IT15	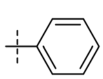	—	27.21	12.22	N.D.	N.A.

Table 2 (*Contd.*)

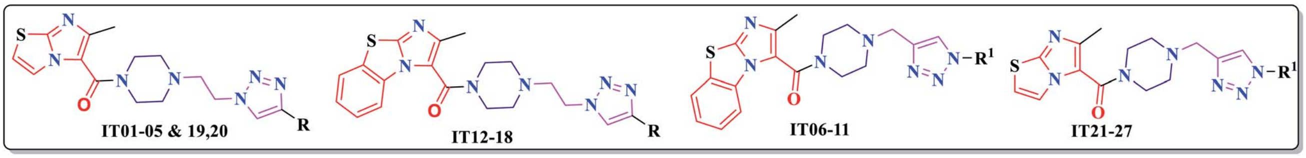

Cmpd.	R	R[1]	Mtb H37Ra[lux a] IC$_{90}$ (μM)	Mtb H37Ra[lux a] IC$_{50}$ (μM)	MRC-5[b] CC$_{50}$ (μM)	T.I.[c] CC$_{50}$/IC$_{50}$
IT16	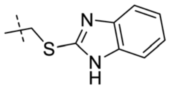	—	14.49	7.09	58.09	8.2
IT17	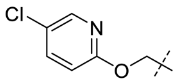	—	115.57	19.74	N.D.	N.A.
IT18	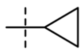	—	63.77	29.13	N.D.	N.A.
IT19	—	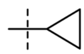	>128	>128	N.D.	N.A.
IT20	—	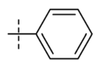	54.94	20.59	N.D.	N.A.
IT21	—	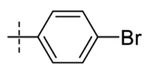	53.02	20.67	N.D.	N.A.
IT22	—	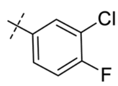	57.82	5.28	N.D.	N.A.
IT23	—	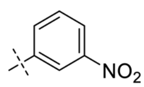	84.83	43.82	N.D.	N.A.
IT24	—	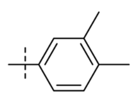	48.78	19.83	N.D.	N.A.
IT25	—	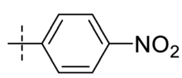	51.36	23.05	N.D.	N.A.
IT26	—	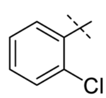	62.14	30.16	N.D.	N.A.
IT27	—	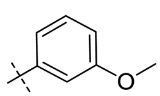	98.08	46.03	N.D.	N.A.
INH[d]			0.09	0.04	N.D.	N.A.
Tamoxifen[e]			N.D.	N.D.	12.40	

[a] MIC and IC$_{50}$ concentrations calculated from the growth inhibition of 90% and 50%, respectively, based on luminometry of cultures exposed to a 10-point serial dilution in triplicate. The experiment was followed by two independent repeats. Percentage inhibitions >10% were repeated. [b] Viability of MRC-5 fibroblast cell line cultures, measured as a 50% reduction in fluorescence in a resazurin assay. [c] T.I., the therapeutic index calculated by dividing the CC$_{50}$ by the IC$_{50}$. INH, isoniazid a first-line TB drug used as reference drug. Tamoxifen, a reference compound for cellular toxicity. [d] N.D = Not determined. [e] N.A = Not applicable.

effectiveness was calculated as the minimal inhibitory concentration (MIC) at which the mycobacterial growth is reduced by 90% as well as the IC$_{50}$, in which 50% of mycobacterial growth was reduced, as reported in Table 2. Within the series, hits were defined during profiling as test compounds that reached an MIC against Mtb H37Ra^{lux} below 15 μM. Albeit arbitrary by nature, the selected stringency was chosen based on the overall potency of the series. Out of the compound library, nine hits were selected, meeting the outlined criteria. The nine compounds include three derivatives (**IT02–IT04**) from the imidazo-[2,1-*b*]-thiazole cluster with MIC between 10.22 μM and 14.59 μM and six derivatives from the benzo-[*d*]-imidazo-[2,1-*b*]-thiazole cluster (**IT08–IT11**, **IT13** and **IT16**) with MIC between 7.05 μM and 14.49 μM. These nine compounds were selected for a study of potential acute cellular toxicity as reported in Table 2. As a cellular model for acute toxicity, the human MRC-5 fibroblast cell line was selected.[59] The cell line was exposed to the synthesized derivatives for 24 h after which viability was measured. Viability was detected by the addition of Resazurin, a non-toxic, cell-permeable purple dye which is reduced in living cells to a pink, highly fluorescent resorufin.[60] The acute cytotoxic concentration of the test compounds was defined as the concentration at which the cells failed to reduce 50% of Resazurin compared to the non-exposed negative control cells. For the tested derivatives, acute toxicity could only be detected at concentration tenfold higher than the IC_{50} towards Mtb H37Ra^{lux}. For three benzo-[*d*]-imidazo-[2,1-*b*]-thiazole derivatives (**IT08–IT10**) and one imidaz-[2,1-*b*]-thiazole derivative **IT04**, a reduction in viability following exposure was not observed altogether at 128 μM. By dividing the CC_{50} with the IC_{50}, the Therapeutic Index (T.I.) can be calculated to allow the selection of the derivative with the most favourable activity. From this analysis, the 4-nitro phenyl substituted benzo-[*d*]-imidazo-[2,1-*b*]-thiazole derivative **IT10** showed best activity with an observed IC_{90} of 7.05 μM and an acute cytotoxicity CC_{50} >128 μM.

To discriminate between the potency of the compounds against slow *versus* fast growing mycobacteria, the synthesized benzo-[*d*]-imidazo-[2,1-*b*]-thiazole derivatives with an observed MIC >15 μM against Mtb H37Ra were tested against a panel of non-tuberculous mycobacteria (NTM). The panel of NTM included two members of the *Mycobacterium avium* complex (MAC), *M. avium* subsp. *avium* and *M. intracellulare.*[61] Both MAC species cause TB-like pulmonary infections in patients that are immuno-compromised or suffer from severe lung disease. Both species are considered slow growing mycobacteria with a generation time of (10–12 h) similar to the generation time of Mtb (20–24 h). As a model for fast growing mycobacteria, *Mycobacterium smegmatis* and *Mycobacterium abscessus* were selected.[62,63] *M. smegmatis* is considered a non-pathogenic microorganism that infrequently causes opportunistic infections while *M. abscessus* can cause chronic lung disease in vulnerable hosts as well as skin infections in immune deficient patients. *M. abscessus* infections appear to be on the rise, and outbreaks have been observed in hospitals and clinical settings around the world. Both species are considered fast-growing mycobacteria with a shorter generation time of 3 to 4 h. In general, we observed a significantly reduced potency of the (benzo-[*d*])-imidazo-[2,1-*b*]-thiazole derivatives against all NTMs as shown in Table 3. Apart from the 4-*t*-butyl phenyl substituted benzo-imidazo-[2,1-*b*]-thiazole derivative **IT13**, no IC_{50} was observed for any tested compound below 100 μM against the slow growing MAC species. Against the fast-growing NTMs, most derivatives showed activity against the fast-growing *M. smegmatis* but not against *M. abscessus*. Surprisingly, the most active compound out of the Mtb screen (benzo-[*d*])-imidazo-[2,1-*b*]-thiazole derivative **IT10** showed no activity >128 μM against any NTM tested within the panel.

Table 3 Antimycobacterial results of the synthesized imidazo-[2,1-*b*]-thiazole and benzo-[*d*]-imidazo-[2,1-*b*]-thiazole derivatives against a panel of NTMs[a]

	IC_{50} (μM)			
Cmpd.	*M. avium* subsp. *avium*	*M. intracellulare*	*M. smegmatis*	*M. abscessus*
IT02	125.8	119.3	>128.0	>128.0
IT03	>128.0	63.4	28.2	>128.0
IT04	>128.0	>128.0	16.4	>128.0
IT08	>128.0	>128.0	44.1	>128.0
IT09	>128.0	>128.0	5.7	>128.0
IT10	>128.0	>128.0	>128.0	>128.0
IT11	100.2	98.8	52.7	>128.0
IT13	17.1	>128.0	34.6	>128.0
IT16	123.5	>128.0	103.2	>128.0

[a] IC_{50} concentrations calculated from the growth inhibition 50% based on luminometry of cultures exposed to a 10-point serial dilution in triplicate. The experiment was followed by two independent repeats. Percentage inhibitions >10% were repeated.

2.4 Molecular docking studies

The crystal structure of Mtb pantothenate synthetase (PDB-3IUB) was retrieved from the RCSB Protein Data Bank[56] (**https://www.rcsb.org/structure/3iub**) with a resolution of 1.5 Å. After importation, the protein was prepared by Schrödinger Protein Preparation Wizard and a grid was generated. The co-crystal ligand **FG-2** was extracted/removed from the PDB structure, re-docked in the generated grid, and checked for superimposition. The Root-mean-square deviation (RMSD) was found to be 0.22 Å, indicating that the docking protocol was validated and suitable for the docking study (Fig. 4) of the test molecules.

Molecular docking is one of the widely used structure based drug design (SBDD) techniques in computer-aided drug design approach. It is useful in drug discovery to predict the predominant binding mode(s) of a test ligand with a target protein of

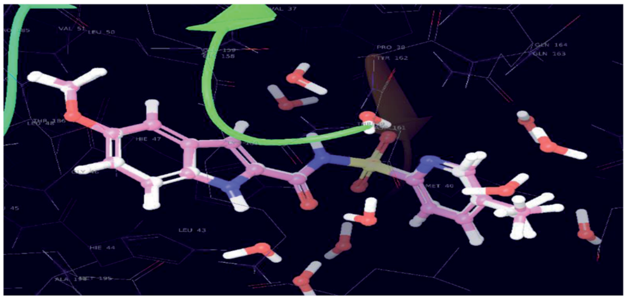

Fig. 4 Superimposed view of the native orientation of ligand **FG-2** (X-ray crystallized pose) and docked orientation of the same ligand in the active site of the protein (3IUB) (Root mean square deviation 0.22 Å) (color interpretation—pink color—binding pose after docking, white color—X-ray native pose of ligand).

Table 4 Docking results and interactions of the test compounds (**FG-2**, **IT06**, **IT10**)

S. no.	Code	Hydrogen-bond	Aromatic bond	Pi–Pi interactions	Glide score (kcal mol^{-1})
1	Co-crystal ligand (**FG-2**)	MET-40 GLN-164 HIS-47 VAL-187	HIS-47 GLN-164 MET-195	HIS-44 (Pi–Pi stacking)	−4.96
2	**IT06**	HIS-44	GLN-164 MET-195	VAL-187 (halogen bond) HIS-47	−1.95
3	**IT10**	VAL-187 SER 197	MET-195	ARG 198 (2) HIS-44	−1.29

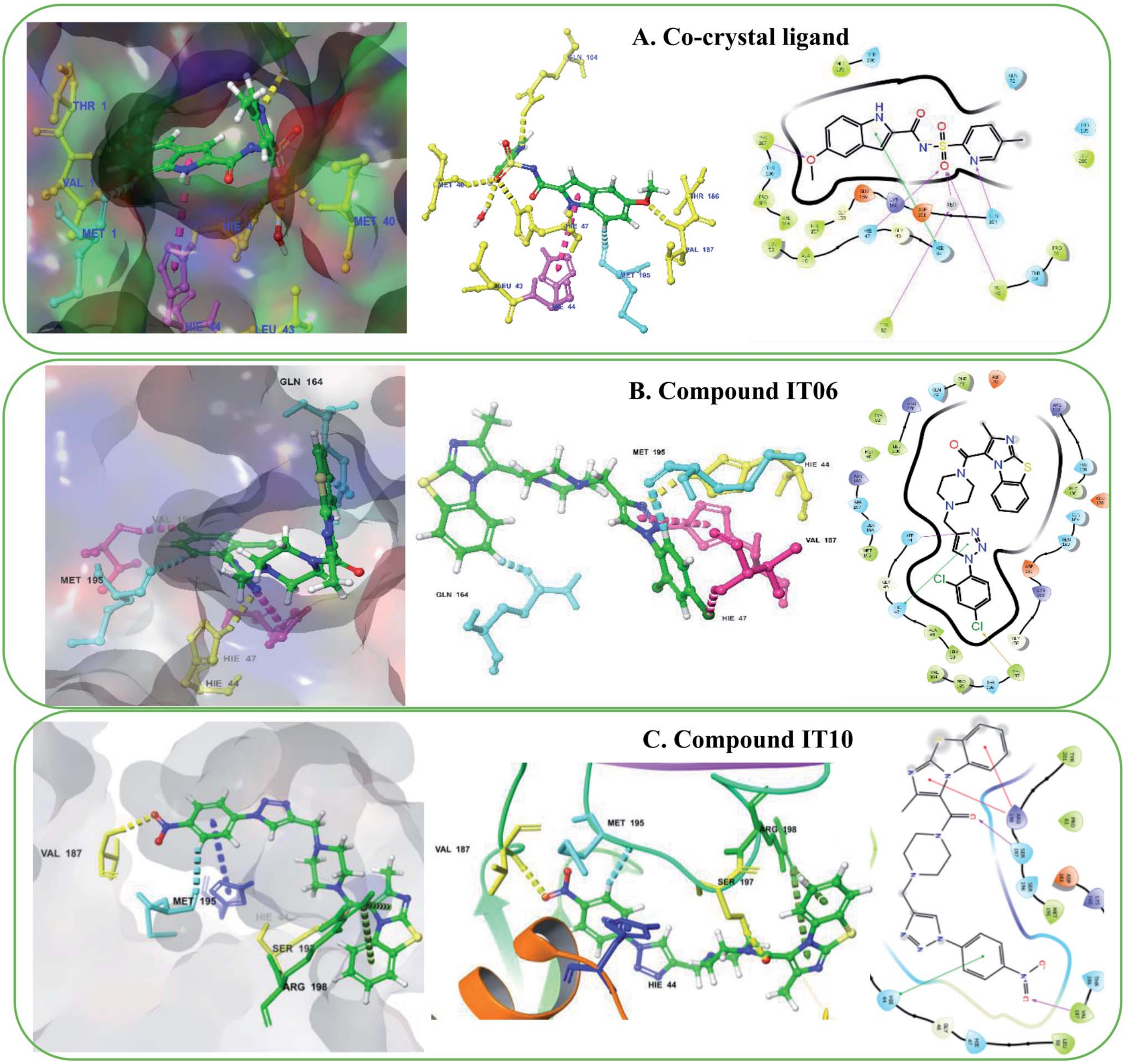

Fig. 5 (A) Docked orientations (3D and 2D) of the co-crystal ligand (**FG-2**) in the active site of the protein (3IUB). (B) Docked orientations (3D and 2D) of the significantly active compound **(IT06)** in the active site of the protein (3IUB) C. Docked orientations (3D and 2D) of the significantly active compound **(IT10)** in the active site of the protein (3IUB) (*color interpretation of amino acid residues—yellow hydrogen bond. Blue aromatic bond, pink Pi interactions, yellow halogen bond interaction (2D)*).

a known three-dimensional structure. In the current study also, in order to identify the variety of orientations, conformations, and interactions exhibited by the significantly active molecule, a docking study was initially carried out on an exemplar molecules, analog **IT06** and **IT10**, followed by the docked poses were critically analyzed using an XP visualizer. The docking scores and the nature of interactions exhibited by the co-crystal ligand and test molecules are depicted in Table 4. By scrutinizing the co-crystal ligand's (**FG-2**) 3D and 2D (Fig. 5) poses, amino acid residues MET-40, HIS-47 and VAL-187, GLN-164 contributed their part in hydrogen bond formation with the co-crystal ligand and showed the docking score of -4.96 kcal mol^{-1}. Apart from the hydrogen bond interactions, the co-crystal ligand also exhibited three aromatic bonds with HIS-47, MET-195, and GLN-164 amino-acid residues. HIS-44 amino-acid residue revealed pi–pi stacking interaction with the co-crystal ligand. Interestingly, one water molecule was also involved in the hydrogen bond formation with the ligand in the active site of the target.

When the selected model compound **IT06** was subjected to docking at the active site of the target protein, many interactions were observed. The amino acid HIS-44 was involved in the hydrogen bond interactions with the test compound **IT06.** In terms of aromatic interactions, GLN-164 and MET-195 were found common as that of co-crystal ligand. Additionally, one halogen bond was exhibited with a chlorine atom of phenyl triazole nucleus. Another compound **IT10** also revealed two hydrogen bond interactions with VAL187, SER-197 amino acid residues. Additionally, MET-195 exposed an aromatic bond interaction with the target. Two Pi–Pi interactions were observed with compound **IT10** with the amino acid residue ARG-198, and another with HIS-44. All these interactions made the complex best fit in the active site of the target PS (PDB-3IUB) of Mtb.

2.5 Molecular dynamic studies

The best conformations of each docked pose of co-crystal ligand and significantly active compounds **IT06**, **IT10** were subjected to a molecular dynamics (MD) simulation study to examine the stability of the protein and ligand complex (PLC).

Here, we analyzed the binding energy between target enzyme and ligand, the structural changes during complex docking, and interactions of salt bridges and hydrogen bonds. An excellent root mean square deviation (RMSD) was found for the co-crystal ligand (Fig. 6). Critical analysis was carried out to check the stability of the enzyme and co-crystal ligand; at the initial stage of the molecular dynamics, around 15 ns, minor instability was revealed. After the simulation started around 20 ns, the enzyme and co-crystal ligand were in close contact. Molecular docking and molecular dynamics studies both revealed the same amino acids involved in various types of interactions. The same amino acids, for instance, VAL-187, were wholly involved in the hydrogen bond interaction throughout the simulation. Apart from this, HIS-44, HIS-47, LYS-160, VAL-187, MET-195, SER-196 and SER-197 residues actively participated in hydrogen bond interactions with the co-crystal ligand at the active site of the target PS (PDB-3IUB) of Mtb (Fig. 7). In the same way, 49% to 99% of the MD simulated contacts were found with the co-crystal ligand FG-2. Furthermore, the SER-197 residue contributed a continuous contact of 99% throughout with an oxygen atom of the SO_2 group of the ligand, and the indole nitrogen atom of the ligand collaborated 98% with the MET-195 residue of the protein. During amino-acid residue interactions analysis, water-mediated interactions were also identified. All these interactions made the complex stable during the entire duration of the study.

The significantly active compound **IT06** was also analyzed with the molecular dynamics simulation to confirm its conformational changes occurring during the simulation. The protein and the compound **IT06** ligand complex were analyzed by checking RMSD. After critical analysis of the compound **IT06,** results were acceptable as a 2.8 Å distance was observed between protein and **IT06** ligand complex. The amino acids HIS-44 and GLN-164 highly contributed to the hydrogen bond interaction with the protein and **IT06** ligand. The same amino acids were involved in the interactions during molecular docking studies also. With these inferences, the protein and compound **IT06** ligand fits perfectly in the active site of the target PS (PDB-3IUB) of Mtb. GLN-164 amino-acid residue exposed 94% of the interaction with the carbonyl oxygen of

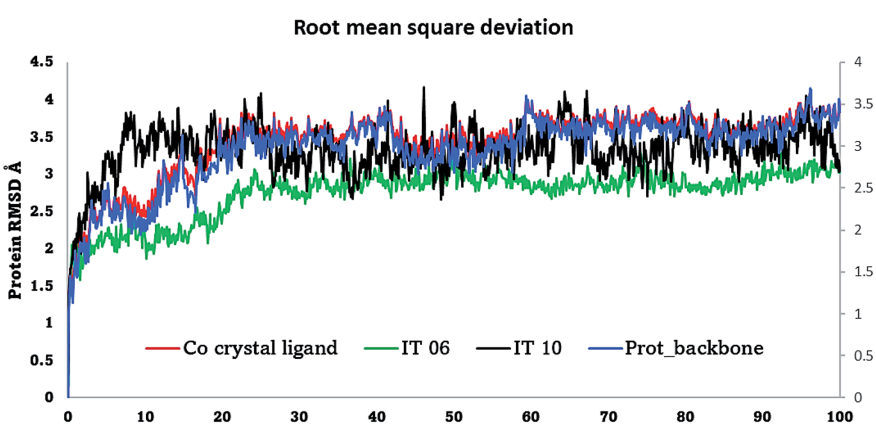

Fig. 6 Root mean square deviation (RMSD) of the co-crystal ligand **FG-2**, compound IT06 and compound IT10 complexes.

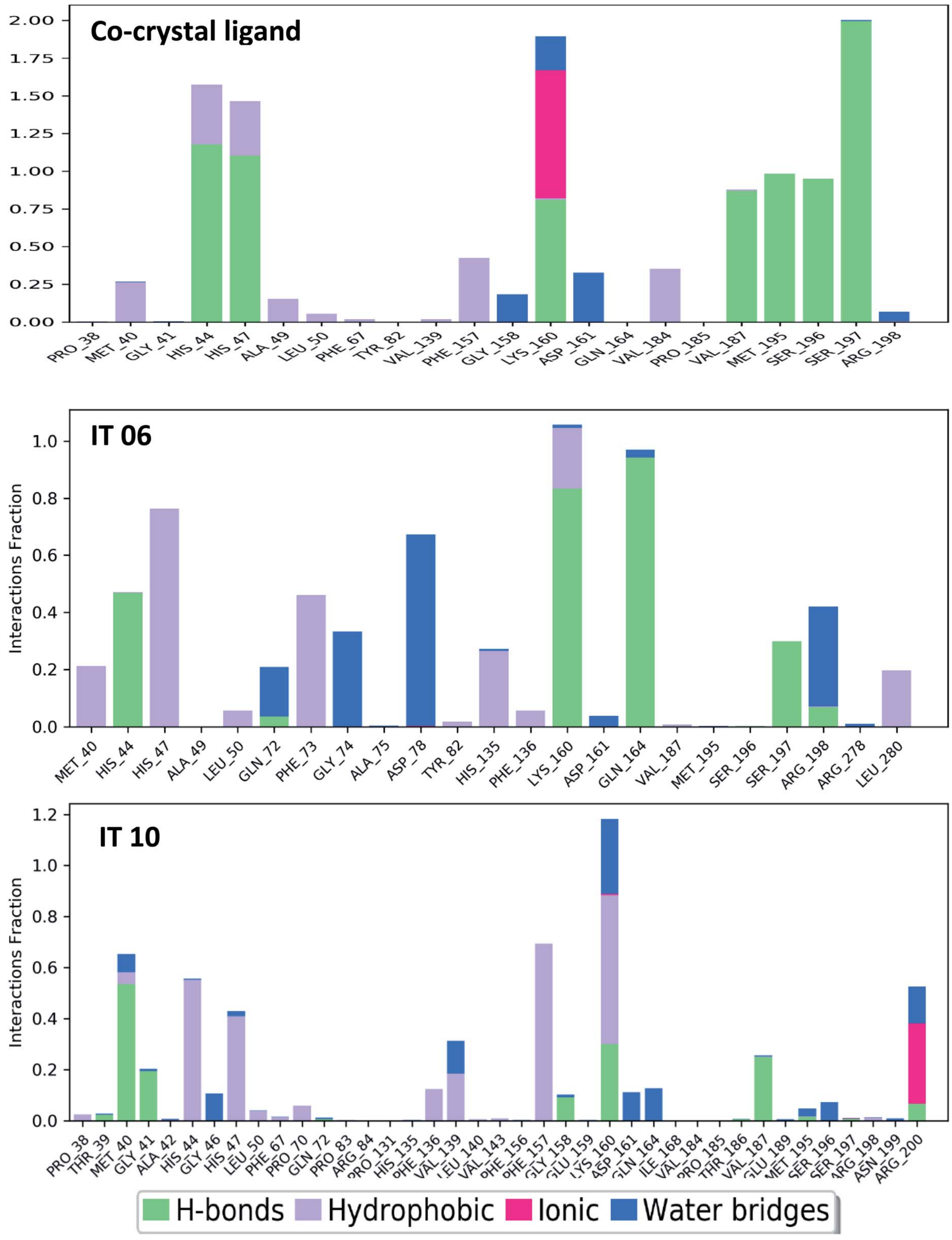

Fig. 7 Protein ligand histogram of the co-crystal ligand **FG-2**, compound **IT06** and compound **IT10** complexes.

piperidinoyl group. The phenyl triazole moiety divulged two hydrogen bond interactions with HIS-44 (46%) and SER-197 (29%) amino acid residues (Fig. 8). All these simulations gave insights for future studies.

The investigation was continued to another protein-ligand complex **IT10.** The conformational changes of the ligand was observed up to 20 ns. After 20 ns, the **IT10** complex was observed stable with slight fluctuations that were within the

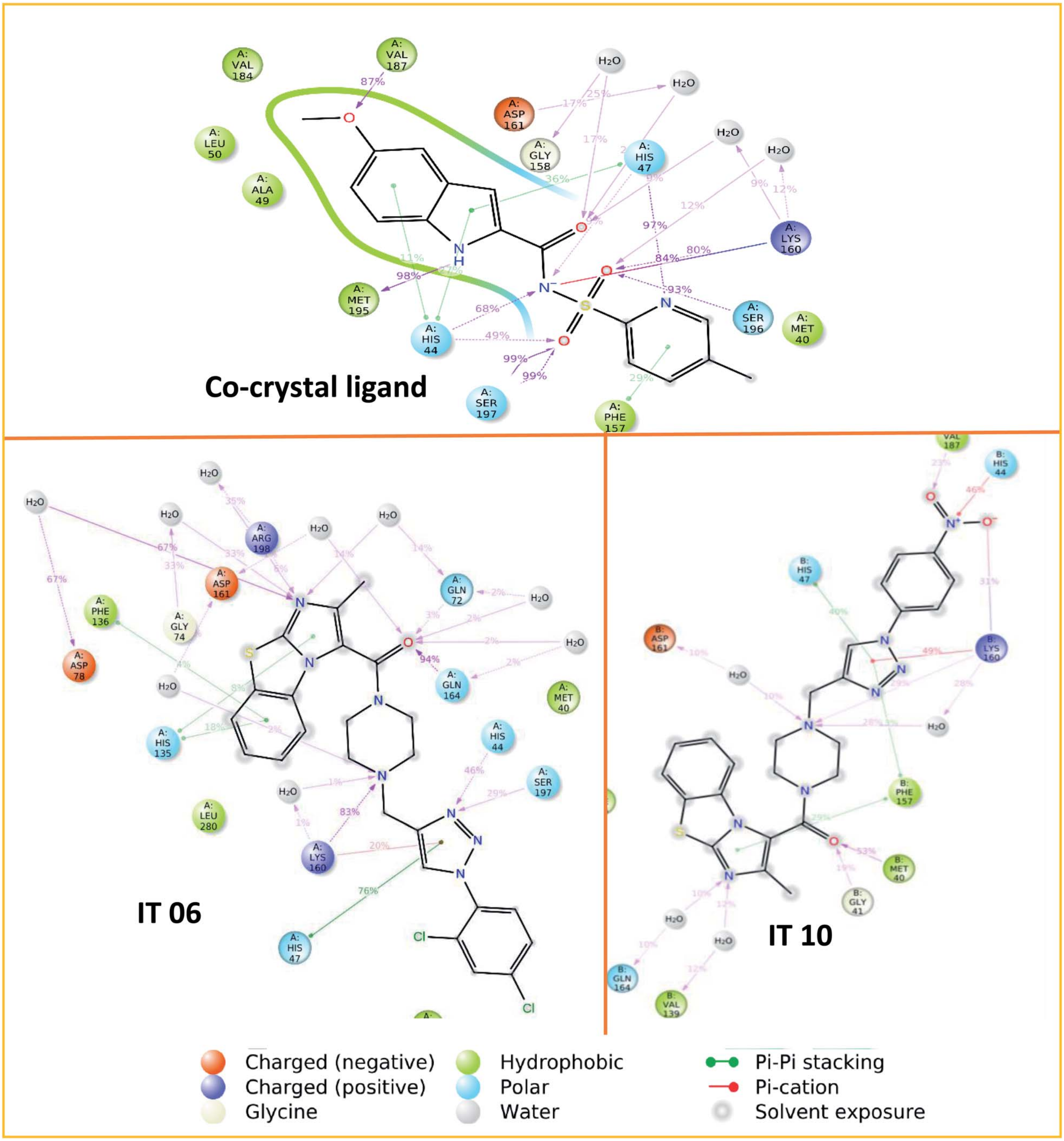

Fig. 8 Percentage of amino-acid residue interactions with the co-crystal ligand **FG-2**, compound **IT06** and compound **IT10** complexes.

range. The hydrogen bond interaction observed in the molecular docking studies with the amino acid residue VAL 187 revealed the same in the histogram of the molecular dynamics studies as well. The nitro group of the **IT10** was contributed to the pi interaction with the amino acid residue HIS44 (46%). The keto group also involved in the active hydrogen bond formation with MET40 (53%). Another amino acid residue of the target LYS 160 (49%) was actively collaborated with the triazine moiety of the ligand **IT10** with pi interaction. Overall, the molecular dynamics studies of the selected ligands were perfectly fitted in the active site of the target of PS from *Mycobacterium tuberculosis*.

3 Conclusion

A panel of around twenty-seven imidazo-[2,1-*b*]-thiazole (**IT01-IT05** and **IT19-IT27**) and benzo-[*d*]-imidazo-[2,1-*b*]-thiazole (**IT06-IT18**) derivatives were designed, *in silico* ADMET predicted, synthesized in a straightforward approach by the combination of piperazine and various 1,2,3-triazole analogues. Admittedly, the potency of the synthesized panel towards Mtb was fairly low which led to arbitrary hit selection of >15 μM with the best compound selected, derivative **IT10**. Substitution at position 4 with a nitro phenyl moiety, as accomplished in compound **IT10**, lowered the observed IC_{90} of the benzo-[*d*]-imidazo-[2,1-*b*]-thiazole scaffold to 7.05 μM and IC_{50} of 2.32 μM and removed observable acute cellular toxicity >128 μM against MRC-5 lung fibroblast cell line. Another benzo-[*d*]-imidazo-[2,1-*b*]-thiazole compound (**IT06**) holding 2,4-dichloro phenyl moiety also exhibited significant activity (IC_{50} 2.03 μM) against the tested strain of *Mycobacterium tuberculosis.* The observed activity confirms the antitubercular activity and the versatility of the imidazo-[2,1-*b*]-thiazoles as a potential pharmacophore. The flexibility of the scaffold should enable a straightforward library enrichment that could allow an in-depth structure activity relation (SAR) study and lead to more active library members based on the scaffolding design strategy. The low or absent toxicity towards the MRC-5 fibroblast cell line and the significantly reduced activity towards various NTM species potentially points towards a highly selective inhibitory activity exerted by the tested panel. In order to find the putative binding mode of the significantly active molecule and stability of protein-ligand complex, molecular docking and molecular dynamics studies were carried out at the active site of Pantothenate synthetase (PDB-3IUB).

4 Experimental section

4.1 Chemistry: general procedure for preparation of intermediates and final compounds

The general procedure of preparation of intermediates and final compounds is detailed in the ESI† section.

4.1.1 (4-(2-(4-Butyl-1*H*-1,2,3-triazol-1-yl)-ethyl)-piperazin-1-yl)(6-methylimidazo-[2,1-*b*]-thiazol-5-yl)-methanone (IT01). Brown gummy solid, yield 82%, ^{1}H NMR (400 MHz, DMSO-d_6) δ 7.86 (s, 1H), 7.76 (d, J = 4.4 Hz, 1H), 7.30 (d, J = 4.4 Hz, 1H), 4.44 (t, J = 6.4 Hz, 2H), 3.55 (t, J = 6.4 Hz, 4H), 2.78 (t, J = 6.4 Hz, 2H), 2.60 (t, J = 7.5 Hz, 2H), 2.49–2.43 (m, 4H), 2.29 (s, 3H), 1.63–1.51 (m, 2H), 1.36–1.28 (m, 2H), 0.89 (t, J = 7.4 Hz, 3H); ^{13}C NMR (101 MHz, DMSO-d_6) δ 161.55, 150.33, 147.08, 144.90, 122.57, 120.70, 118.00, 113.89, 57.29, 52.92, 47.02, 45.28, 31.61, 29.48, 25.13, 22.55, 22.08, 15.71, 14.41, 14.15. ESI MS (*m*/*z*): calcd for $C_{19}H_{27}N_7OS$: 401.20, found 402 $[M + H]^+$; anal. calcd for $C_{19}H_{27}N_7OS$: (%) C, 56.83; H, 6.78; N, 24.42; found: C, 56.85; H, 6.75; N, 24.41.

4.1.2 (4-(2-(4-(4-(*tert*-Butyl)phenyl)-1*H*-1,2,3-triazol-1-yl)-ethyl)-piperazin-1-yl)(6-methylimidazo-[2,1-*b*]-thiazol-5-yl)-methanone (IT02). Pale yellow solid, M.P.: 62–64 °C, Yield 75%, ^{1}H NMR ^{1}HNMR (400 MHz, DMSO-d_6): δ 8.52 (s, 1H), 7.77 (t, J = 2.0 Hz, 2H), 7.75 (d, J = 1.9 Hz, 1H), 7.47 (d, J = 2.0 Hz, 1H), 7.46–7.45 (t, J = 2.9 Hz, 1H), 7.29 (d, J = 4.4 Hz, 1H), 4.54 (t, J = 6.2 Hz, 2H), 3.51 (t, 4H), 2.86 (t, J = 6.1 Hz, 2H), 2.56–2.51 (m, 4H), 2.29 (s, 3H), 1.30 (s, 9H); ^{13}C NMR (101 MHz, DMSO-d_6) δ 161.63, 153.08, 150.71, 146.56, 128.62, 126.08, 125.38, 121.86, 120.75, 113.89, 57.18, 52.92, 47.29, 45.29, 34.82, 31.54, 29.47, 15.82. ESI MS (*m*/*z*): calcd for $C_{25}H_{31}N_7OS$: 477.23, found 478 $[M + H]^+$; anal. calcd for $C_{19}H_{27}N_7OS$: (%) C, 62.87; H, 6.54; N, 20.53; found: C, 62.89; H, 6.52; N, 20.54.

4.1.3 (6-Methylimidazo-[2,1-*b*]-thiazol-5-yl)(4-(2-(4-nonyl-1*H*-1,2,3-triazol-1-yl)-ethyl)-piperazin-1-yl)-methanone (IT03). Pale yellow gammy solid, yield 86%, ^{1}H NMR (400 MHz, DMSO-d_6) δ 7.91 (s, 1H), 7.81 (d, J = 4.4 Hz, 1H), 7.38 (d, J = 4.4 Hz, 1H), 4.48 (t, J = 6.4 Hz, 2H), 3.57 (t, 4H), 2.78 (t, J = 6.4 Hz, 2H), 2.60 (t, J = 7.5 Hz, 2H), 2.49–2.43 (m, 4H), 2.35 (m, 9H), 1.63–1.51 (m, 4H), 1.36–1.28 (m, 4H), 0.92 (t, J = 7.4 Hz, 3H); ^{13}C NMR (101 MHz, DMSO-d_6) δ 161.53, 150.39, 147.12, 144.92, 122.61, 120.73, 118.12, 113.91, 57.31, 52.95, 47.08, 45.34, 31.59, 29.48, 28.31, 27.91, 27.23, 26.41, 26.12, 25.13, 22.55, 22.08, 15.71, 14.41, 14.15. ESI MS (*m*/*z*): calcd for $C_{24}H_{37}N_7OS$: 471.28, found 472 $[M + H]^+$; anal. calcd for $C_{24}H_{37}N_7OS$: (%) C, 61.12; H, 7.91; N, 20.79; found: C, 61.15; H, 7.93; N, 20.76.

4.1.4 (4-(2-(4-(((1*H*-Benzo-[*d*]-imidazole-2-yl)-thio)-methyl)-1*H*-1,2,3-triazol-1-yl)-ethyl)-piperazin-1-yl)(6-methylimidazo-[2,1-*b*]-thiazol-5-yl)-methanone (IT04). Pale yellow solid, M.P.: 65–67 °C, Yield 79%, ^{1}HNMR (400 MHz, DMSO-d_6): δ 12.81 (s, 1H), 8.06 (s, 1H), 7.78 (s, 1H), 7.44 (m, 2H), 7.33–7.31 (m, 1H), 7.09 (d, J = 5.9 Hz, 2H), 4.62 (s, 2H), 4.53 (t, J = 3.4 Hz, 2H), 3.46 (t, J = 3.4 Hz, 4H), 2.99 (t, J = 3.6 Hz, 2H), 2.70–2.53 (t, J = 3.6 Hz, 4H), 2.28 (s, 3H); ^{13}C NMR (101 MHz, DMSO-d_6) δ 161.62, 150.46, 149.85, 145.06, 143.68, 124.47, 121.89, 120.73, 118.81, 117.83, 114.00, 52.48, 31.61, 30.29, 29.47, 26.37, 22.56, 15.72. ESI MS (*m*/*z*): calcd for $C_{23}H_{25}N_9OS_2$: 507.16, found 508 $[M + H]^+$; anal. calcd for $C_{23}H_{25}N_9OS_2$: (%) C, 54.42; H, 4.96; N, 24.83; found: C, 54.46; H, 4.98; N, 24.81.

4.1.5 (4-(2-(4-(((5-Chloropyridin-2-yl)-oxy)-methyl)-1*H*-1,2,3-triazol-1-yl)ethyl)-piperazin-1-yl)(6-methylimidazo-[2,1-*b*]-thiazol-5-yl)-methanone (IT05). Brown gammy solid, yield 85%, ^{1}HNMR (400 MHz, DMSO-d_6): δ 8.10 (s, 1H), 8.06 (d, J = 2.8 Hz, 1H), 8.02 (d, J = 2.8 Hz, 1H), 7.76 (d, J = 4.4 Hz, 1H), 7.50 (dd, J = 5.2, 2.9 Hz, 1H), 7.30 (d, J = 4.4 Hz, 1H), 5.13 (s, 2H), 4.48 (t, J = 5.5 Hz, 2H), 3.47 (t, J = 5.5 Hz, 4H), 2.77 (t, J = 6.3 Hz, 2H), 2.47 (t, J = 4.5 Hz, 4H), 2.28 (s, 3H); ^{13}C NMR (101 MHz, DMSO-d_6) δ 161.56, 160.15, 159.79, 142.29, 141.41, 141.14, 137.17, 136.29, 124.97, 121.32, 120.70, 113.91, 110.82, 57.09, 52.84, 47.19, 43.97, 15.72. ESI MS (*m*/*z*): calcd for $C_{21}H_{23}ClN_8O_2S$: 486.14, found 487 $[M + H]^+$ and 509 $[M + Na]^+$; anal. calcd for $C_{21}H_{23}ClN_8O_2S$: C, 51.80; H, 4.76; Cl, 7.28; N, 23.01; found: C, 51.83; H, 4.78; Cl, 7.30; N, 23.03.

4.1.6 (4-((1-(2,4-Dichlorophenyl)-1*H*-1,2,3-triazol-4-yl)-methyl)-piperazin-1-yl)(2-methylbenzo-[*d*]-imidazo-[2,1-*b*]-thiazol-3-yl)-methanone (IT06). Brown gammy solid, yield 85%, ^{1}HNMR (400 MHz, DMSO-d_6): δ 8.46 (s, 1H), 8.32 (s, 1H), 8.03 (dd, J = 8.0, 0.8 Hz, 1H), 7.99 (d, J = 2.1 Hz, 1H), 7.72 (dd, J = 10.0, 8.0 Hz, 2H), 7.52–7.47 (m, 1H), 7.41 (t, J = 7.8, 1.2 Hz, 1H), 3.74 (s, 2H), 3.54 (t, J = 6.5, 1.4 Hz, 2H), 2.70–2.59 (m, 4H), 2.44 (t, J = 6.5, 1.4 Hz, 2H), 2.28 (s, 3H); ^{13}C NMR (101 MHz, DMSO-d_6) δ 160.75, 135.77, 134.14, 132.32, 130.57, 130.25, 130.01, 129.55, 129.05, 126.98, 126.65, 125.37, 114.80, 52.44, 29.46, 15.03: ESI MS (*m*/*z*): calcd for $C_{24}H_{21}Cl_2N_7OS$: 525.09, found 526 $[M + H]^+$ and 548 $[M + Na]^+$; anal. calcd for $C_{24}H_{21}Cl_2N_7OS$: (%) C, 54.76; H, 4.02; Cl, 13.47; N, 18.62; found: C, 54.74; H, 4.05; Cl, 13.49; N, 18.65.

4.1.7 (4-((1-(3-Methoxyphenyl)-1*H*-1,2,3-triazol-4-yl)-methyl)-piperazin-1-yl)(2-methylbenzo-[*d*]-imidazo-[2,1-*b*]-

thiazol-3-yl)-methanone (IT07). Black solid, M.P.: 81–83 °C, yield 70%, ^{1}HNMR (400 MHz, DMSO-d_6): δ 8.76 (s, 1H), 8.02 (d, J = 7.9 Hz, 1H), 7.70 (d, J = 8.1 Hz, 1H), 7.50–7.46 (m, 4H), 7.39 (t, J = 7.2 Hz, 1H), 7.10–7.02 (m, 1H), 3.86 (t, J = 6.9 Hz, 4H), 3.73 (t, J = 6.9 Hz, 4H), 3.55 (s, 2H), 2.65 (s, 3H), 2.29 (s, 3H); ^{13}C NMR (101 MHz, DMSO-d_6) δ 160.96, 160.66, 138.21, 132.37, 131.26, 129.52, 126.94, 125.40, 125.34, 122.67, 114.84, 114.73, 112.35, 111.64, 111.54, 105.96, 105.23, 56.07, 55.79, 52.66, 29.47, 15.17. ESI MS (m/z): calcd for $C_{25}H_{25}N_7O_2S$: 487.18, found 488 $[M + H]^+$ and 510 $[M + Na]^+$; anal. calcd for $C_{25}H_{25}N_7O_2S$: (%) C, 61.58; H, 5.17; N, 20.11; found: C, 61.61; H, 5.19; N, 20.13.

4.1.8 (2-Methylbenzo-[*d*]-imidazo-[2,1-*b*]-thiazol-3-yl)(4-((1-(3-nitrophenyl)-1*H*-1,2,3-triazol-4-yl)-methyl)-piperazin-1-yl)-methanone (IT08). Pale brown solid, M.P.:161–163 °C, Yield 74%, ^{1}HNMR (400 MHz, DMSO-d_6): δ 8.98 (s, 1H), 8.73 (t, J = 2.1 Hz, 1H), 8.41 (dd, J = 8.1, 1.3 Hz, 1H), 8.32 (dd, J = 8.0, 1.5 Hz, 1H), 8.04–8.00 (m, 1H), 7.90 (t, J = 8.1 Hz, 1H), 7.70 (d, J = 7.7 Hz, 1H), 7.48–7.43 (m, 1H), 7.40–7.35 (m, 1H), 3.75 (s, 2H), 3.55 (s, 2H), 2.64 (m, 4H), 2.45 (s, 2H), 2.29 (s, 3H); ^{13}C NMR (101 MHz, DMSO-d_6) δ 160.81, 149.02, 145.12, 137.74, 132.30, 132.00, 129.54, 126.92, 126.41, 125.35, 123.44, 123.11, 115.06, 114.80, 52.61, 29.47, 22.56, 15.03, 14.41. ESI MS (m/z): calcd for $C_{24}H_{22}N_8O_3S$, 502.15, found 503 $[M + H]^+$ and 525 $[M + Na]^+$; anal. calcd for $C_{24}H_{22}N_8O_3S$: (%) C, 57.36; H, 4.41; N, 22.30; found: C, 57.33; H, 4.43; N, 22.28.

4.1.9 (4-((1-(3,4-Dimethylphenyl)-1*H*-1,2,3-triazol-4-yl)-methyl)-piperazin-1-yl)(2-methylbenzo-[*d*]-imidazo-[2,1-*b*]-thiazol-3-yl)-methanone (IT09). Brown gammy solid, yield 78%, ^{1}H NMR (400 MHz, DMSO-d_6) δ 8.64 (s, 1H), 8.32 (s, 1H), 8.02 (d, J = 7.2 Hz, 1H), 7.70 (dd, J = 4.5, 2.4 Hz, 2H), 7.59 (dd, J = 8.1, 2.2 Hz, 1H), 7.49–7.44 (m, 1H), 7.41–7.36 (m, 1H), 7.33 (d, J = 8.2 Hz, 1H), 3.70 (s, 2H), 3.54 (s, 2H), 2.74–2.52 (m, 4H), 2.44 (s, 2H), 2.31 (s, 3H), 2.28 (s, 6H); ^{13}C NMR (101 MHz, DMSO-d_6) δ 160.79, 138.53, 137.30, 135.10, 130.98, 129.54, 126.94, 125.41, 122.37, 121.26, 117.63, 114.79, 52.72, 31.16, 29.48, 22.56, 19.88, 19.43. ESI MS (m/z): calcd for $C_{26}H_{27}N_7OS$: 485.20, found 486 $[M + H]^+$ and 508 $[M + Na]^+$; anal. calcd for $C_{26}H_{27}N_7OS$: (%) C, 64.31; H, 5.60; N, 20.19; found: C, 64.32; H, 5.62; N, 20.16.

4.1.10 (2-Methylbenzo-[*d*]-imidazo-[2,1-*b*]-thiazol-3-yl)(4-((1-(4-nitrophenyl)-1*H*-1,2,3-triazol-4-yl)-methyl)-piperazin-1-yl)-methanone (IT10). Yellow solid, M.P.: 173–175 °C,yield 80%, ^{1}HNMR (400 MHz, DMSO-d_6): δ 8.95 (s, 1H), 8.46 (d, J = 9.0 Hz, 2H), 8.23 (d, J = 9.0 Hz, 2H), 8.02 (d, J = 7.8 Hz, 1H), 7.70 (d, J = 8.2 Hz, 1H), 7.46 (t, J = 7.6 Hz, 1H), 7.39 (t, J = 7.5 Hz, 1H), 3.75 (s, 2H), 3.55 (s, 2H), 2.77–2.57 (m, 4H), 2.46–2.37 (m, 2H), 2.29 (s, 3H); ^{13}C NMR (101 MHz, DMSO-d_6) δ 160.82, 148.33, 147.07, 145.36, 141.38, 132.31, 129.54, 126.93, 126.03, 125.41, 123.10, 120.91, 120.58, 114.82, 112.84, 53.00, 52.55, 47.61, 15.05. ESI MS (m/z): calcd for $C_{24}H_{22}N_8O_3S$: 502.15, found 503 [M + H]+and 525 $[M + Na]^+$; anal. calcd for $C_{24}H_{22}N_8O_3S$: (%) C, 57.36; H, 4.41; N, 22.30; found: C, 57.34; H, 4.43; N, 22.34.

4.1.11 (4-((1-(3-Chlorophenyl)-1*H*-1,2,3-triazol-4-yl)-methyl)-piperazin-1-yl)(2-methylbenzo-[*d*]-imidazo-[2,1-*b*]-thiazol-3-yl)-methanone (IT11). Pale brown solid, M.P.: 132–134 °C, yield 75.4%, ^{1}HNMR (400 MHz, DMSO-d_6): δ 8.82 (s, 1H), 8.05 (s, 1H), 7.93 (d, J = 7.6 Hz, 1H), 7.70 (d, J = 8.0 Hz, 1H), 7.63 (t, J = 8.0 Hz, 1H), 7.56 (d, J = 7.6 Hz, 1H), 7.47 (t, J = 7.6 Hz, 2H), 7.38 (t, J = 7.4 Hz, 1H), 3.75 (s, 2H), 3.55 (t, J = 34.7 Hz, 4H), 2.66 (t, J = 34.7 Hz, 4H), 2.29 (s, 3H); ^{13}C NMR (101 MHz, DMSO-d_6) δ 160.68, 138.22, 134.66, 132.52, 132.08, 131.09, 129.50, 128.80, 126.96, 125.39, 125.35, 122.92, 120.19, 118.97, 114.91, 52.62, 41.99, 31.74, 29.47, 16.63. ESI MS (m/z): calcd for $C_{24}H_{22}ClN_7OS$: 491.13, found 492 $[M + H]^+$ and 514 $[M + Na]^+$; anal. calcd for $C_{24}H_{22}ClN_7OS$: (%) C, 58.59; H, 4.51; Cl, 7.21; N, 19.93; found: C, 58.63; H, 4.55; Cl, 7.19; N, 19.95.

4.1.12 (4-(2-(4-Butyl-1*H*-1,2,3-triazol-1-yl)-ethyl)-piperazin-1-yl)(2-methylbenzo-[*d*]-imidazo-[2,1-*b*]-thiazol-3-yl)-methanone (IT12). Brown gammy solid, Yield 80%, ^{1}H NMR (400 MHz, DMSO-d_6) δ 8.03 (dd, J = 8.0, 0.9 Hz, 1H), 7.86 (s, 1H), 7.73 (dd, J = 5.9, 2.4 Hz, 1H), 7.54–7.49 (m, 1H), 7.44–7.39 (m, 1H), 4.44 (t, J = 6.3 Hz, 2H), 3.58 (t, J = 74.2 Hz, 4H), 2.79 (t, J = 6.2 Hz, 2H), 2.60 (t, J = 7.5 Hz, 4H), 2.28 (s, 3H), 1.60–1.52 (m, 2H), 1.34–1.29 (m, 2H), 1.25–1.22 (m, 2H), 0.88 (dd, J = 8.7, 6.0 Hz, 3H); ^{13}C NMR (101 MHz, DMSO-d_6) δ 160.72, 148.31, 147.07, 144.19, 132.32, 129.53, 127.00, 125.44, 125.35, 122.58, 118.99, 114.87, 57.20, 53.09, 47.01, 31.61, 29.46, 25.13, 22.08, 15.01, 14.15. ESI MS (m/z): calcd for $C_{23}H_{29}N_7OS$: 451.22, found 452 $[M + H]^+$ and 474 $[M + Na]^+$; anal. calcd for $C_{23}H_{29}N_7OS$: (%) C, 61.17; H, 6.47; N, 21.71; found: C, 61.18; H, 6.50; N, 21.75.

4.1.13 (4-(2-(4-(4-(*tert*-Butyl)-phenyl)-1*H*-1,2,3-triazol-1-yl)-ethyl)-piperazin-1-yl)(2-methylbenzo-[*d*]-imidazo-[2,1-*b*]-thiazol-3-yl)-methanone (IT13). Yellow solid, M.P.: 115–117 °C, Yield 77%, ^{1}HNMR (400 MHz, DMSO-d_6): δ 8.52 (s, 1H), 8.04 (d, J = 7.8 Hz, 1H), 7.76 (d, J = 8.3 Hz, 2H), 7.72 (s, 1H), 7.53 (t, J = 7.3 Hz, 1H), 7.46 (d, J = 7.8 Hz, 2H), 7.40 (s, 1H), 4.54 (t, J = 5.8 Hz, 2H), 3.50 (t, J = 5.8 Hz, 4H), 2.86 (t, t, J = 5.8 Hz 2H), 2.60 (t, J = 6.0 Hz, 4H), 2.29 (s, 4H), 1.28 (s, 9H); ^{13}C NMR (101 MHz, DMSO-d_6) δ 161.12, 152.13, 150.72, 146.59, 137.04, 132.66, 131.91, 129.56, 128.60, 127.10, 126.28, 126.07, 125.97, 125.51, 125.39, 121.87, 119.28, 118.00, 115.06, 57.10, 47.31, 34.99, 34.81, 31.53, 31.32, 31.24, 16.34. ESI MS (m/z): calcd for $C_{29}H_{33}N_7OS$, 527.25, found 528 $[M + H]^+$ and 550 $[M + Na]^+$; anal. calcd for $C_{29}H_{33}N_7OS$: (%) C, 66.01; H, 6.30; N, 18.58; found: C, 66.031; H, 6.32; N, 18.62.

4.1.14 (2-methylbenzo-[*d*]-imidazo-[2,1-*b*]-thiazol-3-yl)(4-(2-(4-nonyl-1*H*-1,2,3-triazol-1-yl)-ethyl)-piperazin-1-yl)-methanone (IT14). Yellow gammy solid, yield 88%, ^{1}H NMR (400 MHz, DMSO-d_6) δ 8.12 (dd, J = 8.3, 1.2 Hz, 1H), 7.92 (s, 1H), 7.80 (dd, J = 5.9, 2.4 Hz, 1H), 7.62–7.55 (m, 1H), 7.50–7.42 (m, 1H), 4.46 (t, J = 6.4 Hz, 2H), 3.58–3.50 (t, J = 6.4 Hz, 4H), 2.75 (t, J = 6.4 Hz, 2H), 2.62 (t, J = 7.5 Hz, 2H), 2.45–2.41 (m, 4H), 2.38 (m, 9H), 1.60–1.55 (m, 4H), 1.38–1.3.1 (m, 4H), 0.93 (t, J = 7.4 Hz, 3H); ^{13}C NMR (101 MHz, DMSO-d_6) δ 161.53, 150.39, 147.12, 144.92, 124.78, 124.56, 123.48, 123.12, 122.61, 120.73, 118.12, 113.91, 57.31, 52.95, 47.08, 45.34, 31.59, 29.48, 28.31, 27.91, 27.23, 26.41, 26.12, 25.13, 22.55, 22.08, 15.71, 14.41, 14.15. ESI MS (m/z): calcd for chemical formula: $C_{28}H_{39}N_7OS$: 521.29, found 522 $[M + H]^+$ and 544 $[M + Na]^+$; anal. calcd for $C_{28}H_{39}N_7OS$: (%) C, 64.46; H, 7.53; N, 18.79; found: C, 64.43; H, 7.55; N, 18.80.

4.1.15 (2-Methylbenzo-[*d*]-imidazo-[2,1-*b*]-thiazol-3-yl)(4-(2-(4-phenyl-1*H*-1,2,3-triazol-1-yl)-ethyl)-piperazin-1-yl)-methanone (IT15). Brown solid, M.P.: 107–109, yield 86%, ^{1}HNMR (400 MHz, DMSO-d_6): δ 8.58 (s, 1H), 8.04 (d, J = 7.8 Hz, 1H), 7.85 (d, $J = 7.4$ Hz, 2H), 7.73 (d, $J = 8.0$ Hz, 1H), 7.62 (d, $J = 7.1$ Hz, 1H), 7.45 (t, $J = 7.5$ Hz, 3H), 7.33 (t, $J = 7.1$ Hz, 1H), 4.56 (t, $J = 9.2$ Hz, 2H), 3.52 (t, $J = 11.2$ Hz, 4H), 2.89 (t, $J = 9.2$ Hz, 2H), 2.67 (t, $J = 11.2$ Hz, 4H), 2.31 (s, 3H). ^{13}C NMR (101 MHz, DMSO-d_6) δ 160.71, 146.59, 144.19, 132.31, 131.35, 129.52, 129.37, 128.25, 127.02, 125.59, 125.45, 125.34, 122.16, 114.87, 57.10, 47.33, 29.45, 22.55, 15.01. ESI MS (m/z): calcd for chemical formula: $C_{25}H_{25}N_7OS$: 471.18, found 472 $[M + H]^+$; anal. calcd for $C_{25}H_{25}N_7OS$: (%) C, 63.67; H, 5.34; N, 20.79; found: C, 63.69; H, 5.36; N, 20.82.

4.1.16 (4-(2-(4-((1*H*-Benzo-[*d*]-imidazole-2-yl)-thio)-1*H*-1,2,3-triazol-1-yl)-ethyl)-piperazin-1-yl)(2-methylbenzo-[*d*]-imidazo[2,1-*b*]-thiazol-3-yl)-methanone (IT16). Pale yellow solid, M.P.: 79–81 °C, yield 86%, ^{1}H NMR (400 MHz, DMSO-d_6) δ 12.78 (s, 1H), 8.12 (s, 1H), 8.04 (d, $J = 7.7$ Hz, 1H), 7.73 (d, $J = 8.2$ Hz, 1H), 7.66 (d, $J = 6.0$ Hz, 1H), 7.45–7.40 (m, 2H), 7.15 (d, $J = 7.4$ Hz, 1H), 7.08 (s, 2H), 4.65 (d, $J = 7.3$ Hz, 2H), 4.46 (s, 2H), 3.45 (t, $J = 11.8$ Hz, 4H), 2.75 (s, 2H), 2.54 (t, $J = 11.8$ Hz, 4H), 2.27 (s, 3H); ^{13}C NMR (101 MHz, DMSO-d_6) δ 160.03, 132.41, 129.54, 127.02, 126.01, 125.47, 124.28, 123.34, 123.21, 122.91, 122.13, 121.10, 120.85, 118.48, 114.94, 109.53, 108.92, 106.67, 56.93, 52.97, 47.25, 29.46, 26.51, 24.30, 15.19. ESI MS (m/z): calcd for chemical formula: $C_{27}H_{27}N_9OS_2$: 557.18, found 558 $[M + H]^+$; anal. calcd for $C_{27}H_{27}N_9OS_2$: (%) C, 58.15; H, 4.88; N, 22.60; found: C, 58.19; H, 4.93; N, 22.58.

4.1.17 (4-(2-(4-((5-Chloropyridin-2-yl)oxy)-1*H*-1,2,3-triazol-1-yl)-ethyl)-piperazin-1-yl)(2-methylbenzo-[*d*]-imidazo-[2,1-*b*]-thiazol-3-yl)-methanone (IT17). Brown solid, M.P.: 92–94 °C, yield 76%, ^{1}H NMR (400 MHz, DMSO-d_6): δ 8.32 (s, 1H), 8.10 (s, 1H), 8.05 (d, $J = 2.7$ Hz, 2H), 7.72 (d, $J = 8.2$ Hz, 1H), 7.47–7.39 (m, 3H), 5.13 (s, 2H), 4.47 (t, $J = 5.9$ Hz, 2H), 3.44 (t, $J = 11.2$ Hz, 4H), 2.77 (t, $J = 5.6$ Hz, 2H), 2.28 (t, $J = 11.2$ Hz, 4H), 1.23 (s, 3H). ^{13}C NMR (101 MHz, DMSO-d_6) δ 160.13, 141.11, 137.15, 132.35, 127.02, 125.45, 125.36, 125.00, 121.32, 114.86, 110.80, 57.01, 47.20, 43.94, 29.47, 22.56, 14.41. ESI MS (m/z): calcd for $C_{25}H_{25}ClN_8O_2S$: 536.15, found 537 $[M + H]^+$ and 559 $[M + Na]^+$; anal. calcd for $C_{25}H_{25}ClN_8O_2S$: (%) C, 55.91; H, 4.69; Cl, 6.60; N, 20.87; found: C, 55.93; H, 4.73; Cl, 6.64; N, 20.90.

4.1.18 (4-(2-(4-Cyclopropyl-1*H*-1,2,3-triazol-1-yl)-ethyl)-piperazin-1-yl)(2-methylbenzo-[*d*]-imidazo-[2,1-*b*]-thiazol-3-yl)-methanone (IT18). Yellow solid, M.P.: 77–79 °C, yield 81%, ^{1}H NMR (400 MHz, DMSO-d_6): δ 8.03 (d, $J = 7.8$ Hz, 1H), 7.85 (s, 1H), 7.73 (d, $J = 8.1$ Hz, 1H), 7.52 (t, $J = 7.6$ Hz, 1H), 7.42 (t, $J = 7.5$ Hz, 1H), 4.42 (t, $J = 22.3$ Hz, 2H), 3.64–3.46 (m, 4H), 2.78 (t, $J = 22.3$ Hz, 2H), 2.41–2.20 (m, 4H), 1.96 (m, 1H), 1.25 (s, 3H), 0.88 (d, $J = 6.4$ Hz, 2H), 0.69 (d, $J = 3.1$ Hz, 2H); ^{13}C NMR (101 MHz, DMSO-d_6) δ 160.73, 149.12, 132.34, 129.53, 127.01, 125.44, 125.34, 121.49, 114.89, 57.19, 47.04, 29.47, 22.56, 15.05, 8.08, 7.02. ESI MS (m/z): calcd for $C_{22}H_{25}N_7OS$: 435.18, found 436 $[M + H]^+$; anal. calcd for $C_{22}H_{25}N_7OS$: (%) C, 60.67; H, 5.79; N, 22.51; found: C, 60.64; H, 5.81; N, 22.53.

4.1.19 (4-(2-(4-Cyclopropyl-1*H*-1,2,3-triazol-1-yl)-ethyl)-piperazin-1-yl)(6-methylimidazo-[2,1-*b*]-thiazol-5-yl)-methanone (IT19). Pale yellow gammy solid, yield 84%, ^{1}H NMR (400 MHz, DMSO-d_6) δ 7.84 (d, $J = 2.8$ Hz, 1H), 7.76 (d, $J = 4.4$ Hz, 1H), 7.30 (d, $J = 4.4$ Hz, 1H), 4.41 (t, $J = 6.3$ Hz, 2H), 3.51 (s, 4H), 2.79 (s, 2H), 2.50–2.46 (m, 4H), 2.29 (s, 3H), 1.96–1.90 (m, 1H), 0.91–0.86 (m, 2H), 0.72–0.66 (m, 2H); ^{13}C NMR (101 MHz, DMSO-d_6) δ 161.55, 150.33, 149.13, 144.94, 121.49, 120.71, 118.00, 113.90, 57.21, 52.89, 46.95, 45.19, 15.73, 8.08, 7.02. ESI MS (m/z): calcd for $C_{18}H_{23}N_7OS$: 385.17, found 386 $[M + H]^+$ and 408 $[M + Na]^+$; anal. calcd for $C_{18}H_{23}N_7OS$: (%) C, 56.08; H, 6.01; N, 25.43; found: C, 56.10; H, 6.04; N, 25.48.

4.1.20 (6-Methylimidazo-[2,1-*b*]-thiazol-5-yl)(4-(2-(4-phenyl-1*H*-1,2,3-triazol-1-yl)-ethyl)-piperazin-1-yl)-methanone (IT20). Yellow solid, M.P.: 53–54 °C, yield 68%, ^{1}H NMR (400 MHz, DMSO-d_6): δ 8.58 (s, 1H), 7.85 (d, $J = 7.4$ Hz, 2H), 7.45 (t, $J = 7.4$ Hz, 3H), 7.35–7.29 (m, 2H), 4.56 (t, $J = 5.6$ Hz, 2H), 3.52 (t, $J = 7.8$ Hz, 4H), 2.89 (t, $J = 5.6$ Hz, 2H), 2.55 (t, $J = 7.8$ Hz, 4H), 2.29 (s, 3H); ^{13}C NMR (101 MHz, DMSO-d_6) δ 161.65, 146.60, 132.88, 131.36, 130.51, 129.37, 128.25, 125.59, 122.20, 120.87, 120.77, 113.98, 57.08, 52.88, 47.21, 45.23, 15.86. ESI MS (m/z): calcd for $C_{21}H_{23}N_7OS$: 421.17, found 422 $[M + H]^+$ and 444 $[M + Na]^+$; anal. calcd for $C_{21}H_{23}N_7OS$: (%) C, 59.84; H, 5.50; N, 23.26; found: C, 59.89; H, 5.52; N, 23.29.

4.1.21 (4-((1-(4-Bromophenyl)-1*H*-1,2,3-triazol-4-yl)-methyl)-piperazin-1-yl)(6-methylimidazo-[2,1-*b*]-thiazol-5-yl)-methanone (IT21). Pale brown solid, M.P.: 72–74 °C, yield 83%, ^{1}H NMR (400 MHz, DMSO-d_6) δ 8.77 (s, 1H), 7.90 (d, $J = 8.5$ Hz, 2H), 7.80 (d, $J = 8.6$ Hz, 2H), 7.77 (d, $J = 4.2$ Hz, 1H), 7.29 (d, $J = 4.2$ Hz, 1H), 3.72 (s, 2H), 3.55 (t, $J = 7.5$ Hz, 4H), 2.53 (t, $J = 7.5$ Hz, 4H), 2.30 (s, 3H); ^{13}C NMR (101 MHz, DMSO-d_6) δ 161.59, 150.35, 144.91, 136.36, 133.22, 122.67, 122.33, 121.61, 120.75, 118.02, 113.89, 52.82, 52.71, 45.22, 15.77. ESI MS (m/z): calcd for $C_{20}H_{20}BrN_7OS$: 485.06, found 486 $[M + H]^+$; anal. calcd for $C_{20}H_{20}BrN_7OS$: (%) C, 49.39; H, 4.14; Br, 16.43; N, 20.16; found: C, 49.42; H, 4.16; Br, 16.47; N, 20.20.

4.1.22 (4-((1-(3-Chloro-4-fluorophenyl)-1*H*-1,2,3-triazol-4-yl)-methyl)-piperazin-1-yl)(6-methylimidazo-[2,1-*b*]-thiazol-5-yl)-methanone (IT22). Black solid, M.P.: 97–99 °C, yield 77%, ^{1}H NMR (400 MHz, DMSO-d_6) δ 8.79 (s, 1H), 8.23 (d, $J = 3.4$ Hz, 1H), 7.97 (s, 1H), 7.77 (s, 1H), 7.67 (t, $J = 8.6$ Hz, 1H), 7.30 (s, 1H), 3.73 (s, 2H), 3.55 (t, $J = 6.9$ Hz, 4H), 2.53 (t, $J = 6.8$ Hz, 4H), 2.30 (s, 3H). ^{13}C NMR (101 MHz, DMSO-d_6) δ 161.61, 158.46, 156.00, 150.38, 144.93, 134.15, 123.02, 122.68, 121.30, 121.22, 120.76, 118.70, 118.47, 113.89, 52.79, 52.70, 45.27, 15.79. ESI MS (m/z): calcd for $C_{20}H_{19}ClFN_7OS$: 459.10, found 460 $[M + H]^+$ and 482 $[M + Na]^+$; anal. calcd for $C_{20}H_{19}ClFN_7OS$: (%) C, 52.23; H, 4.16; Cl, 7.71; F, 4.13; N, 21.32; found: C, 52.25; H, 4.19; Cl, 7.68; F, 4.19; N, 21.35.

4.1.23 (6-Methylimidazo-[2,1-*b*]-thiazol-5-yl)(4-((1-(3-nitrophenyl)-1*H*-1,2,3-triazol-4-yl)-methyl)-piperazin-1-yl)-methanone (IT23). Pale yellow solid, M.P.: 104–106 °C, yield 87%, ^{1}H NMR (400 MHz, DMSO-d_6) δ 8.99 (s, 1H), 8.75 (s, 1H), 8.42 (d, $J = 7.3$ Hz, 1H), 8.32 (d, $J = 7.1$ Hz, 1H), 7.90 (t, $J = 7.8$ Hz, 1H), 7.76 (d, $J = 3.0$ Hz, 1H), 7.30 (s, 1H), 3.74 (s, 2H), 3.56 (s, 4H), 2.54 (s, 4H), 2.30 (s, 3H); ^{13}C NMR (101 MHz, DMSO-d_6) δ 161.61, 157.28, 150.36, 149.02, 145.23, 137.75, 132.00, 126.43, 123.44, 123.15, 120.75, 118.06, 115.09, 113.87, 52.81, 52.70, 45.29, 15.79. ESI MS (m/z): calcd for $C_{20}H_{20}N_8O_3S$: 452.14, found 453 $[M + H]^+$; anal. calcd for $C_{20}H_{20}N_8O_3S$: (%) C, 53.09; H, 4.46; N, 24.76; found: C, 53.11; H, 4.48; N, 24.79.

4.1.24 (4-((1-(3,4-Dimethylphenyl)-1*H*-1,2,3-triazol-4-yl)-methyl)-piperazin-1-yl)(6-methylimidazo-[2,1-*b*]-thiazol-5-yl)-

methanone (IT24). Brown solid, M.P.: 52–54 °C, yield 83%, ^{1}H NMR (400 MHz, DMSO-d_6) δ 8.65 (s, 1H), 7.77 (d, J = 4.0 Hz, 1H), 7.71 (s, 1H), 7.61 (d, J = 8.0 Hz, 1H), 7.33 (d, J = 8.2 Hz, 1H), 7.29 (d, J = 4.4 Hz, 1H), 3.70 (s, 2H), 3.55 (t, J = 7.5 Hz, 4H), 2.52 (t, J = 7.5 Hz, 4H), 2.32 (s, 3H), 2.28 (s, 6H); ^{13}C NMR (101 MHz, DMSO-d_6) δ 161.79, 155.67, 144.57, 138.53, 137.29, 135.11, 130.98, 130.57, 126.36, 122.38, 121.26, 120.78, 117.63, 116.91, 113.86, 112.80, 52.84, 45.30, 19.88, 19.42, 18.85, 15.83. ESI MS (m/z): calcd for $C_{22}H_{25}N_7OS$: 435.18, found 436 [M + H]$^+$; anal. calcd for $C_{22}H_{25}N_7OS$: (%) C, 60.67; H, 5.79; N, 22.51; found: C, 60.69; H, 5.81; N, 22.55.

4.1.25 (6-Methylimidazo-[2,1-*b*]-thiazol-5-yl)(4-((1-(4-nitrophenyl)-1*H*-1,2,3-triazol-4-yl)-methyl)-piperazin-1-yl)-methanone (IT25). Brown solid, M.P.: 71–73 °C, yield 87%, ^{1}HNMR (400 MHz, DMSO-d_6): δ 8.97 (s, 1H), 8.45 (d, J = 7.7 Hz, 2H), 8.24 (d, J = 7.8 Hz, 1H), 8.14 (s, 1H), 7.86 (s, 1H), 7.62 (s, 1H), 3.74 (s, 2H), 3.55 (t, J = 7.2 Hz, 4H), 2.44 (t, J = 7.2 Hz, 4H), 2.29 (s, 3H). ^{13}C NMR (101 MHz, DMSO-d_6) δ 190.48, 159.10, 144.68, 143.78, 141.24, 134.68, 133.21, 127.65, 127.18, 126.66, 119.81, 119.15, 114.79, 76.86, 48.39, 46.80, 44.76, 39.23, 30.73. ESI MS (m/z): calcd for $C_{20}H_{20}N_8O_3S$: 452.14, found 453 [M + H]$^+$; anal. calcd for $C_{20}H_{20}N_8O_3S$: (%) C, 53.09; H, 4.46; N, 24.76; found: C, 53.11; H, 4.49; N, 24.72.

4.1.26 (4-((1-(2-Chlorophenyl)-1*H*-1,2,3-triazol-4-yl)-methyl)-piperazin-1-yl)(6-methylimidazo-[2,1-*b*]-thiazol-5-yl)-methanone (IT26). Pale brown solid, M.P.: 106–108 °C, yield 91%, ^{1}HNMR (400 MHz, DMSO-d_6): δ 8.47 (s, 1H), 7.80–7.75 (m, 2H), 7.70 (dd, J = 7.5, 1.4 Hz, 1H), 7.61 (m, 2H), 7.30 (d, J = 4.4 Hz, 1H), 3.75 (s, 2H), 3.55 (t, J = 6.5 Hz, 4H), 2.54 (t, J = 6.5 Hz, 4H), 2.30 (s, 3H). ^{13}C NMR (101 MHz, DMSO-d_6) δ 161.62, 150.34, 144.94, 143.45, 135.10, 132.04, 131.00, 129.01, 128.91, 126.64, 120.71, 118.02, 113.89, 52.74, 52.53, 45.27, 15.75. ESI MS (m/z): calcd for $C_{20}H_{20}ClN_7OS$: 441.11, found 442 [M + H]$^+$; anal. calcd for $C_{20}H_{20}ClN_7OS$: (%) C, 54.36; H, 4.56; Cl, 8.02; N, 22.19; found: C, 54.39; H, 4.58; Cl, 8.06; N, 22.21.

4.1.27 (4-((1-(3-Methoxyphenyl)-1*H*-1,2,3-triazol-4-yl)-methyl)-piperazin-1-yl)(6-methylimidazo-[2,1-*b*]-thiazol-5-yl)-methanone (IT27). Brown solid, M.P.: 67–69 °C, yield 84%, ^{1}H NMR (400 MHz, DMSO-d_6) δ 8.77 (s, 1H), 7.78 (s, 1H), 7.49 (s, 3H), 7.29 (s, 1H), 7.05 (s, 1H), 3.86 (t, J = 7.4 Hz, 4H), 3.72 (s, 2H), 3.55 (t, J = 7.4 Hz, 4H), 2.30 (s, 3H); ^{13}C NMR (101 MHz, DMSO-d_6) δ 161.68, 160.66, 144.70, 138.21, 131.26, 122.71, 120.80, 114.75, 113.90, 112.36, 105.96, 56.08, 52.82, 45.23, 15.83. ESI MS (m/z): calcd for $C_{21}H_{23}N_7O_2S$: 437.16, found 438 [M + H]$^+$; anal. calcd for $C_{21}H_{23}N_7O_2S$: (%) C, 57.65; H, 5.30; N, 22.41; found: C, 57.68; H, 5.32; N, 22.45.

Conflicts of interest

Authors declare that there is no conflict of interest.

Acknowledgements

KVGCS gratefully acknowledge support from the Council of Scientific and Industrial Research, New Delhi (CSIR) (F. No. 02(392)/21/EMR II) and DST-FIST (F. No. SR/FST/CSI-240/2012), New Delhi, India. Central analytical lab facilities of BITS Pilani Hyderabad Campus are gratefully acknowledged. BKK is thankful to the Ministry of Tribal Affairs, Government of India, for the financial assistance (award no. 201920-NFST-TEL-01497). BKK and SM are also grateful to BITS Pilani, Pilani campus for offering research facilities to perform computational simulations. The research conducted by K. V. C., P. C. and D. C. is supported by the Research foundation Flanders (FWO) under grant number G066619N.

References

1 Global tuberculosis reports 2020 by world health organization (WHO).
2 F. Varaine, M. L. Rich, A. Elizabeth, B. Cancedda, S. Keshavjee, C. Mitnick, J. Mukherjee, A. Peruski, K. Seung, E. Ardizzoni, S. Baert, S. Balkan, K. Day, P. Ducros, G. Ferlazzo, C. Ferreyra, M. Gale, P. Hepple, M. Henkens, C. Hewison, N. Hurtado, F. Jochims, J. Rigal, J. Roy, P. Saranchuk, C. V. Gulik, C. Z. Ruffinen, *Tuberculosis: Practical guide for clinicians, nurses, laboratory technicians and medical auxiliaries*, 2022.
3 E. Torfs, T. Piller, P. Cos and D. Cappoen, *Int. J. Mol. Sci.*, 2019, **20**, 1–23.
4 R. J. Cremlyn, 1996, pp. 1–264, ISBN no. 978-0-471-95512-2.
5 A. R. Katritzky, J. Wu, S. Rachwal, B. Rachwal, D. W. Macomber and T. P. Smith, *Org. Prep. Proced. Int.*, 1992, **24**, 463–467.
6 J. Hultén, N. M. Bonham, U. Nillroth, T. Hansson, G. Zuccarello, A. Bouzide, J. Åqvist, B. Classon, U. H. Danielson, A. Karlén, I. Kvarnström, B. Samuelsson and A. Hallberg, *J. Med. Chem.*, 1997, **40**, 885–897.
7 P. Dauban and R. H. Dodd, *Org. Lett.*, 2000, **2**, 2327–2329.
8 I. R. Greig, M. J. Tozer and P. T. Wright, *Org. Lett.*, 2001, **3**, 369–371.
9 M. D. McReynolds, J. M. Dougherty and P. R. Hanson, *Chem. Rev.*, 2004, **104**, 2239–2258.
10 A. Andreani, M. Granaiola, A. Leoni, A. Locatelli, R. Morigi and M. Rambaldi, *Eur. J. Med. Chem.*, 2001, **36**, 743–746.
11 S. Cascioferro, B. Parrino, G. L. Petri, M. G. Cusimano, D. Schillaci, V. Di Sarno, S. Musella, E. Giovannetti, G. Cirrincione and P. Diana, *Eur. J. Med. Chem.*, 2019, **167**, 200–210.
12 G. Çapan, N. Ulusoy, N. Ergenç and M. Kiraz, *Monatshefte Fur Chemie*, 1999, **130**, 1399–1407.
13 A. Andreani, M. Rambaldi and A. Locatelli, *Pharm. Acta Helv*, 1995, **70**, 325–328.
14 A. Andreani, S. Burnelli, M. Granaiola, A. Leoni, A. Locatelli, R. Morigi, M. Rambaldi, L. Varoli, N. Calonghi, C. Cappadone, G. Farruggia, M. Zini, C. Stefanelli, L. Masotti, N. S. Radin and R. H. Shoemaker, *J. Med. Chem.*, 2008, **51**, 809–816.
15 J. S. Barradas, M. I. Errea, N. B. D'Accorso, C. S. Sepúlveda and E. B. Damonte, *Eur. J. Med. Chem.*, 2011, **46**, 259–264.
16 N. S. Shetty, I. A. M. Khazi and C. Ahn, *Bull. Korean Chem. Soc.*, 2010, **31**, 2337–2340.
17 B. A. Bhongade, S. Talath, R. A. Gadad and A. K. Gadad, *J. Saudi Chem. Soc*, 2016, **20**, S463–S475.

18 A. Andreani, M. Rambaldi, A. Locatelli, A. Cristoni, S. Malandrino and G. Pifferi, *Acta Pharm. Nord*, 1992, **4**, 93–96.

19 A. Andreani, M. Rambaldi, A. Leoni, A. Locatelli, R. Bossa, M. Chiericozzi, I. Galatulas and G. Salvatore, *Eur. J. Med. Chem.*, 1996, **31**, 383–387.

20 A. Katiyar, B. Metikurki, S. Prafulla, S. Kumar, S. Kushwaha, D. Schols, E. De Clercq and S. S. Karki, *Acta Pol Pharm*, 2016, **73**, 937–947.

21 A. Andreani, M. Rambaldi, P. Carloni, L. Greci and P. Stipa, *J. Heterocycl. Chem.*, 1989, **26**, 525–529.

22 T. H. Al-Tel, R. A. Al-Qawasmeh and R. Zaarour, *Eur. J. Med. Chem.*, 2011, **46**, 1874–1881.

23 A. Kamal, F. Sultana, M. J. Ramaiah, Y. V. V. Srikanth, A. Viswanath, C. Kishor, P. Sharma, S. N. C. V. L. Pushpavalli, A. Addlagatta and M. Pal-Bhadra, *ChemMedChem*, 2012, **7**, 292–300.

24 M. Palkar, M. Noolvi, R. Sankangoud, V. Maddi, A. Gadad and L. V. G. Nargund, *Arch. Pharm.*, 2010, **343**, 353–359.

25 I. R. Ager, A. C. Barnes, G. W. Danswan, P. W. Hairsine, D. P. Kay, P. D. Kennewell, S. S. Matharu, P. Miller, P. Robson, D. A. Rowlands, W. R. Tully and R. Westwood, *J. Med. Chem.*, 1988, **31**, 1098–1115.

26 M. S. Christodoulou, F. Colombo, D. Passarella, G. Ieronimo, V. Zuco, M. De Cesare and F. Zunino, *Bioorg. Med. Chem.*, 2011, **19**, 1649–1657.

27 A. Andreani, M. Granaiola, A. Leoni, A. Locatelli, R. Morigi, M. Rambaldi, L. Varoli, D. Lannigan, J. Smith, D. Scudiero, S. Kondapaka and R. H. Shoemaker, *Eur. J. Med. Chem.*, 2011, **46**, 4311–4323.

28 C. Blackburn, M. O. Duffey, A. E. Gould, B. Kulkarni, J. X. Liu, S. Menon, M. Nagayoshi, T. Vos and J. Williams, *Bioorg. Med. Chem. Lett.*, 2010, **20**, 4795–4799.

29 H. K. Patel, R. M. Grotzfeld, A. G. Lai, S. A. Mehta, Z. V. Milanov, Q. Chao, K. G. Sprankle, T. A. Carter, A. M. Velasco, M. A. Fabian, J. James, D. K. Treiber, D. J. Lockhart, P. P. Zarrinkar and S. S. Bhagwat, *Bioorg. Med. Chem. Lett.*, 2009, **19**, 5182–5185.

30 G. C. Moraski, N. Deboosère, K. L. Marshall, H. A. Weaver, A. Vandeputte, C. Hastings, L. Woolhiser, A. J. Lenaerts, P. Brodin and M. J. Miller, *PLoS One*, 2020, **15**, 1–19.

31 E. Gürsoy, E. D. Dincel, L. Naesens and N. Ulusoy Güzeldemirci, *Bioorg. Chem.*, 2020, **95**, 103496.

32 G. Samala, P. B. Devi, S. Saxena, N. Meda, P. Yogeeswari and D. Sriram, *Bioorg. Med. Chem.*, 2016, **24**, 1298–1307.

33 G. C. Moraski, N. Seeger, P. A. Miller, A. G. Oliver, H. I. Boshoff, S. Cho, S. Mulugeta, J. R. Anderson, S. G. Franzblau and M. J. Miller, *ACS Infect. Dis.*, 2016, **2**, 393–398.

34 M. H. Shaikh, D. D. Subhedar, L. Nawale, D. Sarkar, F. A. Kalam Khan, J. N. Sangshetti and B. B. Shingate, *MedChemComm*, 2015, **6**, 1104–1116.

35 S. Singireddi, A. Nandikolla, S. Amaroju, A. K. Ewa, A. Głogowska, B. Ghosh, K. K. Banoth, M. Sankaranarayanan, S. Pulya, H. Aggarwal and V. G. C. S. Kondapalli, *Bioorg. Chem.*, 2020, **100**, 103955.

36 P. Shanmugavelan, S. Nagarajan, M. Sathishkumar, A. Ponnuswamy, P. Yogeeswari and D. Sriram, *Bioorg. Med. Chem. Lett.*, 2011, **21**, 7273–7276.

37 B. Zhou, Y. He, X. Zhang, J. Xu, Y. Luo, Y. Wang, S. G. Franzblau, Z. Yang, R. J. Chan, Y. Liu, J. Zheng and Z. Y. Zhang, *Proc. Natl. Acad. Sci. U. S. A.*, 2010, **107**, 4573–4578.

38 D. Addla, A. Jallapally, D. Gurram, P. Yogeeswari, D. Sriram and S. Kantevari, *Bioorg. Med. Chem. Lett.*, 2014, **24**, 1974–1979.

39 T. Yempala, J. P. Sridevi, P. Yogeeswari, D. Sriram and S. Kantevari, *Eur. J. Med. Chem.*, 2014, **71**, 160–167.

40 D. Kumar, Beena, G. Khare, S. Kidwai, A. K. Tyagi, R. Singh and D. S. Rawat, *Eur. J. Med. Chem.*, 2014, **81**, 301–313.

41 C. Menendez, F. Rodriguez, A. L. D. J. L. Ribeiro, F. Zara, C. Frongia, V. Lobjois, N. Saffon, M. R. Pasca, C. Lherbet and M. Baltas, *Eur. J. Med. Chem.*, 2013, **69**, 167–173.

42 C. Menendez, A. Chollet, F. Rodriguez, C. Inard, M. R. Pasca, C. Lherbet and M. Baltas, *Eur. J. Med. Chem.*, 2012, **52**, 275–283.

43 G. Samala, P. B. Devi, S. Saxena, N. Meda, P. Yogeeswari and D. Sriram, *Bioorg. Med. Chem.*, 2016, **24**, 1298–1307.

44 S. Amaroju, M. N. Kalaga, S. Srinivasarao, A. Napiórkowska, E. Augustynowicz-Kopeć, S. Murugesan, S. Chander, R. Krishnan and K. V. G. C. Sekhar, *New J. Chem.*, 2016, **41**, 347–357.

45 A. W. Hung, H. L. Silvestre, S. Wen, G. P. C. George, J. Boland, T. L. Blundell, A. Ciulli and C. Abell, *ChemMedChem*, 2016, **11**, 38–42.

46 A. W. Hung, H. L. Silvestre, S. Wen, A. Ciulli, T. L. Blundell and C. Abell, *Angew. Chem., Int. Ed.*, 2009, **48**, 8452–8456.

47 A. Suresh, S. Srinivasarao, Y. M. Khetmalis, S. Nizalapur, M. Sankaranarayanan and K. V. G. C. Sekhar, *RSC Adv.*, 2020, **10**, 37098–37115.

48 P. S. Girase, S. Dhawan, V. Kumar, S. R. Shinde, M. B. Palkar and R. Karpoormath, *Eur. J. Med. Chem.*, 2021, **210**, 112967.

49 S. Satish, R. Chitral, A. Kori, B. Sharma, J. Puttur, A. A. Khan, D. Desle, K. Raikuvar, A. Korkegian, E. A. F. Martis, K. R. Iyer, E. C. Coutinho, T. Parish and S. Nandan, *Mol. Divers*, 2022, **26**, 73–96.

50 B. Mekonnen Sanka, D. Mamo Tadesse, E. Teju Bedada, E. T. Mengesha and N. Babu G, *Bioorg. Chem.*, 2022, **119**, 105568.

51 A. Nandikolla, S. Srinivasarao, Y. M. Khetmalis, B. K. Kumar, S. Murugesan, G. Shetye, R. Ma, S. G. Franzblau and K. V. G. C. Sekhar, *Toxicol. In Vitro*, 2021, **74**, 105137.

52 D. Lagorce, L. Bouslama, J. Becot, M. A. Miteva and B. O. Villoutreix, *Bioinformatics*, 2017, **33**, 3658–3660.

53 A. Daina, O. Michielin and V. Zoete, *Sci. Rep.*, 2017, **7**, 1–13.

54 S. Chander, P. Ashok, D. Cappoen, P. Cos and S. Murugesan, *Chem. Biol. Drug Des.*, 2016, **88**, 585–591.

55 J. J. Li, D. D. Holsworth and L. Y. Hu, *Chemtracts*, 2003, **16**, 439–442.

56 S. K. Burley, H. M. Berman, C. Bhikadiya, C. Bi, L. Chen, L. Di Costanzo, C. Christie, K. Dalenberg, J. M. Duarte, S. Dutta, Z. Feng, S. Ghosh, D. S. Goodsell, R. K. Green, V. Guranović, D. Guzenko, B. P. Hudson, T. Kalro,

Y. Liang, R. Lowe, H. Namkoong, E. Peisach, I. Periskova, A. Prlić, C. Randle, A. Rose, P. Rose, R. Sala, M. Sekharan, C. Shao, L. Tan, Y. P. Tao, Y. Valasatava, M. Voigt, J. Westbrook, J. Woo, H. Yang, J. Young, M. Zhuravleva and C. Zardecki, *Nucleic Acids Res.*, 2019, **47**, D464–D474.

57 M. B. de Macedo, R. Kimmel, D. Urankar, M. Gazvoda, A. Peixoto, F. Cools, E. Torfs, L. Verschaeve, E. S. Lima, A. Lyčka, D. Milićević, A. Klásek, P. Cos, S. Kafka, J. Košmrlj and D. Cappoen, *Eur. J. Med. Chem.*, 2017, **138**, 491–500.

58 D. Cappoen, E. Torfs, T. Meiresonne, P. Claes, E. Semina, F. Holvoet, M. B. de Macedo, F. Cools, T. Piller, A. Matheeussen, K. Van Calster, G. Caljon, P. Delputte, L. Maes, O. Neyrolles, N. De Kimpe, S. Mangelinckx and P. Cos, *Eur. J. Med. Chem.*, 2019, **181**, 111549.

59 J. P. Jacobs, C. M. Jones and J. P. Baille, *Nature*, 1970, **227**, 168–170.

60 J. O'Brien, I. Wilson, T. Orton and F. Pognan, *Eur. J. Biochem.*, 2000, **267**, 5421–5426.

61 C. L. Daley, *Microbiol. Spectrum*, 2017, **5**, 5.2.29.

62 T. Joseph Antony Sundarsingh, J. Ranjitha, A. Rajan and V. Shankar, *J. Infect. Public Health*, 2020, **13**, 1255–1264.

63 L. Strnad and K. L. Winthrop, *Semin. Respir. Crit. Care Med.*, 2018, **39**, 362–376.